



PACIFIC EARTHQUAKE ENGINEERING RESEARCH CENTER

Structural Engineering Reconnaissance of the August 17, 1999, Kocaeli (Izmit), Turkey, Earthquake

Halil Sezen

University of California, Berkeley

Kenneth J. Elwood

University of California, Berkeley

Andrew S. Whittaker

University of California, Berkeley

Khalid M. Mosalam

University of California, Berkeley

John W. Wallace

University of California, Los Angeles

John F. Stanton

University of Washington

Structural Engineering Reconnaissance of the August 17, 1999 Earthquake: Kocaeli (Izmit), Turkey

Halil Sezen

University of California, Berkeley

Kenneth J. Elwood

University of California, Berkeley

Andrew S. Whittaker

(formerly of University of California, Berkeley)
State University of New York at Buffalo

Khalid M. Mosalam

University of California, Berkeley

John W. Wallace

University of California, Los Angeles

John F. Stanton

University of Washington

PEER Report 2000/09
Pacific Earthquake Engineering Research Center
College of Engineering
University of California, Berkeley
December 2000

ABSTRACT

In late August and early September 1999, a team of structural engineers representing the Pacific Earthquake Engineering Research (PEER) Center traveled to Turkey to study damaged and



1

undamaged buildings, bridges, industrial facilities, and lifeline infrastructure affected by the August 17, 1999, Izmit earthquake. The PEER reconnaissance team sought to improve the understanding of the *performance* of the built environment and to identify gaps in a PEER research agenda that is developing knowledge and design tools for performance-based earthquake engineering.

The M_w 7.4 earthquake occurred on the North Anatolian fault in northwestern Turkey at 3:02 a.m. local time. The hypocenter of the earthquake was located near Izmit, 90 km east of Istanbul. Official figures placed the loss of life at approximately 17,225, with more than 44,000 injured. Approximately 77,300 homes and businesses were destroyed and 245,000 more were damaged. The total direct loss was estimated to be more than US\$ 6 billion.

Chapter 1 of this report overviews the general seismicity of the area affected by the earthquake. Chapter 2 reviews briefly the practice of building seismic design and construction in the region, confirming that the construction of reinforced concrete buildings without special details for ductile response (by far the most prevalent form of construction in the epicentral region) was permitted up to the time of the earthquake. The performance of reinforced concrete frame and wall buildings is presented in some detail in Chapter 3. Chapter 4 presents information on the performance of industrial facilities including electrical substations, a petrochemical plant, and an oil refinery. The performance of these facilities during the August 17 earthquake could be considered to be representative of that of industrial facilities of a similar age (1960s and 1970s) in the United

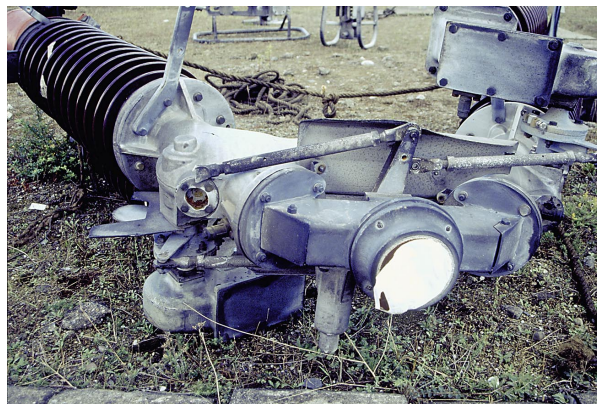
Chapter 1 of this report overviews the general seismicity of the area affected by the



2 3



States and Europe. Chapter 5 summarizes and concludes with brief recommendations related to seismic design practices and performance-based earthquake engineering practice.



- 1 Large permanent drift in weak first story of reinforced concrete building
- 2 Collapsed and damaged reinforced concrete apartment buildings in Degirmendere
- 3 Fault trace through naval station building
- 4 PEER reconnaissance team in front of damaged fertilizer plant tanks
- 5 Damaged fertilizer plant storage tanks
- 6 Damaged electrical substation equipment
- 7 Aerial view of Tüpras refinery
- 8 Flooding and damage resulting from sinking coastline near Gölcük
- 9 Soil-bearing capacity failure

ACKNOWLEDGMENTS

The PEER reconnaissance team included the authors of this report and four representatives of the PEER Business and Industry Partnership (BIP): Mr. Atila Zekioglu of Ove Arup and Partners, Los Angeles, California; Messrs. Jay Love and Chris Smith of Degenkolb Engineers, California; and Dr. Nesrin Basoz of K2 Technologies, San Jose, California. The contributions of these expert design professionals to the reconnaissance effort are gratefully acknowledged. Mss. Janine Hannel and Claire Johnson carefully edited the report and their assistance is also acknowledged.

The PEER reconnaissance team received substantial advice and logistical support from faculty at universities in Turkey. This advice and support was most graciously provided at an exceedingly difficult and demanding time for expert engineers in Turkey. Special thanks are due to Professor Polat Gulkan of the Middle East Technical University, and the faculty at the Department of Civil Engineering at Bogaziçi University including Professors Gulay Altay, Nuray Aydinoglu, Sami Kilic, Emre Otay, and Ali Atilgan. Messrs. Husamettin Danis of Tüpras, Nuri Duzgoren of KordSA, Dursun Parlak of EnerjiSA, Tamer Unlu of ToyotaSA, Ahmet Bilgic of Petkim, Ahmet Akdag of SEKA, and Carey Terrell of DuPont, provided access, assistance, and information to the team during the reconnaissance of selected industrial facilities. The efforts of these individuals and their staffs are gratefully acknowledged.

Two representatives of the Miami-Dade County Urban Search and Rescue Team, Messrs. Robert Sullivan, P.E., and Fred Stolaski, P.E., provided much logistical support and technical advice to the reconnaissance team. Messrs. Sullivan and Stolaski were air-lifted into the epicentral region immediately after the earthquake under orders from the Office of Foreign Disaster Assistance to aid local officials in the search and recovery effort. The PEER reconnaissance team joined with Messrs. Sullivan and Stolaski to survey the epicentral region for the United States State Department. The United States Air Force (Captain Don Treanor) and the United States Marine Corps (Major Coke) provided logistical support for the mission. The helicopters were flown by pilots and crew from the Marine Corps from the USS Kersage, which was diverted from its Kosovo mission by Presidential Order. The PEER reconnaissance team sincerely thanks Messrs. Sullivan and Stolaski, Captain Treanor and Major Coke, and the Air Force and the Marine Corps for their invaluable assistance.

Finally, the senior authors (Whittaker, Mosalam, Wallace, and Stanton) owe a debt of thanks to Professor Sozen of Purdue University. In addition to providing advice and information to the PEER reconnaissance team, Professor Sozen spent significant time with Berkeley graduate students Halil Sezen and Ken Elwood when they first arrived in Turkey, in advance of the remainder of the PEER reconnaissance team. The time spent with Professor Sozen was an opportunity of a lifetime for our two graduate students and they learned much from Professor Sozen in a short period of time. Also, the graduate-student authors (Sezen and Elwood) would like to thank their thesis advisor Professor J. P. Moehle, PEER Center Director, for his patience and understanding during the preparation of this report.

The work described in this report made use of the Pacific Earthquake Engineering Research Center shared facilities supported by the Earthquake Engineering Centers Program of the National Science Foundation under Award Number EEC-9701568.

CONTENTS

ABSTRACT.....	iii
ACKNOWLEDGMENTS	v
TABLE OF CONTENTS.....	vii
LIST OF FIGURES	xi
LIST OF TABLES.....	xv
1 INTRODUCTION	1
1.1 1999 Izmit Earthquake	1
1.2 Seismological and Geotechnical Aspects.....	1
1.3 Scope and Organization of Report	3
2 EVOLUTION OF SEISMIC BUILDING DESIGN PRACTICE IN TURKEY.....	9
2.1 Introduction	9
2.2 Major Earthquakes in Turkey in the 20th Century.....	10
2.3 Building Code Requirements for Reinforced Concrete.....	11
2.4 Seismic Design Codes	11
2.4.1 Years 1940 to 1953.....	11
2.4.2 Years 1954 to 1967.....	12
2.4.3 Years 1968 through 1971.....	13
2.4.4 Years 1972 through 1996.....	15
2.4.5 Years after 1997.....	17
2.5 Comparison of United States and Turkish Codes of Practice	18
2.6 Summary Remarks	19
3 REINFORCED CONCRETE FRAME AND WALL BUILDINGS	29
3.1 Introduction	29
3.2 Construction Practice.....	29
3.3 Moment-Resisting Frame Construction	30
3.3.1 Typical Framing Systems for Residential Construction.....	30
3.3.2 Typical Construction Details	31
3.4 Behavior of Moment-Resisting Frame Construction	32
3.4.1 Moment-Frame Buildings Straddling or Adjacent the Line of Rupture.....	32
3.4.2 Variability of Moment-Frame Building Response	33
3.4.3 Role of Infill Walls in Response of Moment-Frame Buildings.....	33
3.5 Response of Moment-Frame Components	34
3.5.1 Beams	34
3.5.2 Columns.....	34
3.5.3 Beam-Column Joints	35
3.5.4 Asmolen Slab System.....	36
3.6 Shear-Wall Construction	36
3.6.1 Behavior of Shear-Wall Construction	36
3.7 Performance of Selected Buildings	37
3.7.1 Building A	37
3.7.1.1 Building Description	37

3.7.1.2	Component Failures.....	38
3.7.1.3	System Response	38
3.7.2	Building B.....	39
3.7.2.1	Building Description	39
3.7.2.2	Component Failures.....	39
3.7.2.3	System Response	40
3.7.3	Building C.....	40
3.7.3.1	Building Description	40
3.7.3.2	Component Failures.....	41
3.7.3.3	System Response	41
3.7.4	Building D	42
3.7.4.1	Building Description	42
3.7.4.2	System Response	42
3.7.5	Summary Remarks	42
4	INDUSTRIAL FACILITIES	77
4.1	Overview of Construction and Damage	77
4.1.1	Introduction	77
4.1.2	In-Situ Reinforced Concrete Structures.....	81
4.1.3	Prefabricated Reinforced Concrete Structures.....	81
4.1.4	Steel-Frame Structures.....	82
4.2	Petrochemical Industry	82
4.2.1	Introduction	82
4.2.2	Tüpras Refinery	83
4.2.2.1	Introduction	83
4.2.2.2	Loading Jetty	84
4.2.2.3	Tank Farms and Floating Roof Tanks	84
4.2.2.4	Main Processing Facility	85
4.2.3	Petkim Petrochemical Plant.....	86
4.3	Automotive Industry.....	86
4.3.1	Introduction	86
4.3.2	Ford Assembly Plant	87
4.3.3	Hyundai Assembly Plant	87
4.3.4	Toyota Assembly Plant.....	87
4.3.5	Pirelli Tire Plant.....	88
4.3.6	Goodyear Tire Plant.....	88
4.3.7	BekSA.....	88
4.3.8	DuSA	88
4.3.9	KordSA.....	89
4.4	Power Generation and Transmission Systems	89
4.4.1	Introduction	89
4.4.2	Power Generation	89
4.4.3	Power Transmission	90
4.5	Other Heavy Industry	91
4.5.1	Bastas Plant.....	91
4.5.2	Çap Plant.....	91

4.5.3 Habas Plant	91
4.5.4 Mannesmann Boru Plant	92
4.5.5 SEKA Plant.....	92
4.5.6 Liquid Gas Tanks.....	93
5 SUMMARY AND CONCLUSIONS	139
5.1 Summary.....	139
5.2 Conclusions and Recommendations.....	140
APPENDIX PERFORMANCE OF THE ADAPAZARI CITY HALL.....	143
A.1 Introduction	143
A.2 Background Information	143
A.3 1967 Akyazi Earthquake, Damage and Building Retrofit.....	144
A.4 1999 Kocaeli Earthquake and Aftershock.....	145
A.5 Summary Remarks	145
REFERENCES	153

LIST OF FIGURES

Figure 1-1	Map of affected region showing horizontal and vertical offsets	4
Figure 1-2	Vertical offset measured near Ford plant in Gölcük	4
Figure 1-3	Acceleration time histories from the YPT station	5
Figure 1-4	Acceleration response spectra for 5% damping	6
Figure 1-5	Failure of a bridge over the Trans-European Motorway	7
Figure 1-6	Unseating of the simply supported span from the abutment-mounted bearings	7
Figure 1-7	Collapsed and submerged bridge near Akyazi	8
Figure 2-1	Distribution of coefficient C_0 with height above grade in 1961 seismic code.....	21
Figure 2-2	1963 earthquake zonation map (IAEE 1966).....	21
Figure 2-3	Spectral coefficients, S , from 1975 seismic code.....	22
Figure 2-4	Detailing requirements for beams and shear walls from 1975 seismic code	23
Figure 2-5	Detailing requirements for columns from 1975 code.....	24
Figure 2-6	Earthquake zonation map of Turkey (1997 Turkish Seismic Code).....	25
Figure 2-7	Transverse reinforcement requirements for beams (1997 Seismic Code)	25
Figure 2-8	Column confinement zones and detailing requirements (1997 Seismic Code)	26
Figure 2-9	Comparison of elastic response spectra from 1997 UBC and Turkish seismic codes	27
Figure 2-10	Comparison of lateral force coefficient, C , in the 1997 UBC, and 1975 and 1997 Turkish seismic codes	28
Figure 3-1	High-quality apartment building construction in Yalova	44
Figure 3-2	Poor-quality construction of a shear wall in an apartment building in Yalova	44
Figure 3-3	Homeowner apartment building construction	45
Figure 3-4	Construction details for apartment building of Figure 3-3.....	45
Figure 3-5	Typical framing systems in the epicentral region	46
Figure 3-6	Three-story moment-resisting frame east of Gölcük.....	46
Figure 3-7	Floor plan for three-story building of Figure 3-6.....	47
Figure 3-8	Plan of roof framing for a five-story apartment	47
Figure 3-9	Typical modern beam and column rebar details	48
Figure 3-10	Hollow clay tile block used for infill walls	48
Figure 3-11	Asmolen floor system in a four-story building	49
Figure 3-12	Collapse of moment-frame buildings in Gölcük	49
Figure 3-13	Collapsed moment-frame and wall buildings in Adapazari	50
Figure 3-14	Collapsed school building that straddled the line of rupture.....	50
Figure 3-15	Collapsed and damaged moment-frame buildings on the Gölcük naval base.....	51
Figure 3-16	Collapsed building that straddled the line of rupture	51
Figure 3-17	Undamaged building located within 2 m of the line of rupture	52
Figure 3-18	Variability of building response.....	52
Figure 3-19	Varying degrees of damage to infill masonry walls.....	53
Figure 3-20	Damage to infill masonry walls	54
Figure 3-21	Collapsed apartment building in Gölcük.....	54
Figure 3-22	Failure of two stories of a moment-frame building with infill masonry walls	55
Figure 3-23	Formation of a soft and weak story	55
Figure 3-24	Damage to a nonductile reinforced concrete beam	56
Figure 3-25	Failure of lap splices in a moment-frame column.....	56

Figure 3-26	Typical transverse reinforcement details in columns	57
Figure 3-27	Shear failure of a moment-frame blade column.....	57
Figure 3-28	Lack of transverse reinforcement in moment-frame column	58
Figure 3-29	Shear cracking in short columns	58
Figure 3-30	Damage resulting from column-infill masonry wall interaction	59
Figure 3-31	Concentrated damage at ends of moment-frame columns due to drift	59
Figure 3-32	Damage and failures at ends of moment-frame columns	60
Figure 3-33	Damage to moment-frame columns	60
Figure 3-34	Damage to moment-frame beam-column joints.....	61
Figure 3-35	Building collapse due to failure of beam-column joints	61
Figure 3-36	Damage to new moment-frame beam-column joints	62
Figure 3-37	Typical damage to asmlen floor systems	62
Figure 3-38	Shear wall building under construction at the time of the earthquake	63
Figure 3-39	Undamaged apartment building in Gölcük	63
Figure 3-40	Shear wall building damaged due to fault rupture	64
Figure 3-41	Collapsed dual wall-frame building in Adapazari.....	64
Figure 3-42	Damaged wall-frame building due to ground failure and wall rotation	65
Figure 3-43	Damage to short walls or blade columns	66
Figure 3-44	Front elevation of Building A	67
Figure 3-45	Rear elevation of Building A showing intact infill masonry walls	67
Figure 3-46	Building A first-floor plan.....	68
Figure 3-47	Damage to first-story columns	68
Figure 3-48	Damage at the rear stairwell.....	69
Figure 3-49	Shear failure of Column A (see Figure 3-46).....	69
Figure 3-50	Axial failure of Column B (see Figure 3-46)	70
Figure 3-51	Axial failure at the lap splice in Column C (see Figure 3-46)	70
Figure 3-52	Elevation of Building B.....	71
Figure 3-53	Details of damage to the third-story column	71
Figure 3-54	Elevation of Building C.....	72
Figure 3-55	View of retail space in first story of building.....	72
Figure 3-56	Shear crack in first-story column in rear of building	73
Figure 3-57	Damaged beam-column joints at top of first-story columns	73
Figure 3-58	Damaged beam-column joint at top of first-story corner column	74
Figure 3-59	Elevation of Building D	74
Figure 3-60	Settlement of Building D due to liquefaction and soil-bearing failure	75
Figure 4-1	Map of the eastern end of Izmit Bay	94
Figure 4-2	Aerial photograph of industrial facilities in Körfez looking west.....	94
Figure 4-3	Prefabricated reinforced concrete construction.....	95
Figure 4-4	Typical plank roof construction and damaged doveled connections	96
Figure 4-5	Foundation connection for prefabricated reinforced concrete facilities.....	97
Figure 4-6	Damaged precast reinforced concrete framed building.....	98
Figure 4-7	Five-story steel-framed industrial facility under construction	99
Figure 4-8	Tank farm fires at the Tüpras refinery	100
Figure 4-9	Aerial photograph of Tüpras refinery showing part of tank farm	101
Figure 4-10	Aerial photograph of Tüpras refinery.....	101
Figure 4-11	Aerial photograph of loading and unloading jetty at Tüpras refinery	102

Figure 4-12	Failed crude-oil pipeline along the sea wall at the Tüpras refinery	102
Figure 4-13	Photograph from the sea wall of damaged loading and unloading jetty	103
Figure 4-14	Damage to jetty and elevated pipeway at Tüpras refinery	104
Figure 4-15	Tank 211 in Tüpras refinery tank farm	104
Figure 4-16	Floating roof of Tank 211 and spilled oil due to fluid sloshing	105
Figure 4-17	Perimeter seal of floating roof in Tank 211	105
Figure 4-18	Part view of Tüpras tank farm showing Tank 211 and two tank burn zones	106
Figure 4-19	Overtopping of tank wall due to fluid sloshing and failure of perimeter seals	106
Figure 4-20	View of tank wall damage	107
Figure 4-21	Photograph from top of Tank 211 looking approximately south (1 of 2)	107
Figure 4-22	Photograph from top of Tank 211 looking approximately south (2 of 2)	108
Figure 4-23	Photograph of tank destroyed by fire in tank burn zone 1	108
Figure 4-24	Photograph of tank destroyed by fire in tank burn zone 2	109
Figure 4-25	Destroyed walls, walkways, and floating roof of tank of Figure 4-24	109
Figure 4-26	Gross expansion of fixed roof tank adjacent to tank of Figure 4-24	110
Figure 4-27	Photograph of failed 300-ft-tall heater stack	110
Figure 4-28	Damage to heater unit caused by collapse of heater stack	111
Figure 4-29	Damage to pipework caused by collapse of heater stack	111
Figure 4-30	Typical framing in the main processing facility of the Tüpras refinery	112
Figure 4-31	Collapsed wooden cooling tower at the Petkim petrochemical facility	113
Figure 4-32	Damage to nonductile reinforced concrete columns in Petkim cooling tower	113
Figure 4-33	Rebar details and damage in reinforced concrete cooling tower at Petkim	114
Figure 4-34	Loading and unloading port facility at the Petkim petrochemical plant	114
Figure 4-35	Failure of battered reinforced concrete piles beneath jetty at Petkim facility	115
Figure 4-36	Framing of new body shop in Ford plant near Gölcük	115
Figure 4-37	Ground movement near the Ford plant in Gölcük	116
Figure 4-38	Exterior view of the damaged Ford body shop	116
Figure 4-39	Photograph of the BekSA plant	117
Figure 4-40	Damage to the DuSA main plant building	117
Figure 4-41	Photograph of KordSA main building showing steel brace framed tower	118
Figure 4-42	Perimeter of precast reinforced concrete framed DuSA main plant building	118
Figure 4-43	Roof collapse in storage area at KordSA plant	119
Figure 4-44	Rail-mounted transformers in the EnerjiSA transformer yard	119
Figure 4-45	Toppled transformer in EnerjiSA transformer yard	120
Figure 4-46	Heat-recovery steam boiler in the EnerjiSA plant	121
Figure 4-47	Damage to steel framing of the in-service EnerjiSA steam generator	122
Figure 4-48	Damage to steel framing of the new EnerjiSA steam generator	123
Figure 4-49	Aerial photograph of the Adapazari substation	124
Figure 4-50	Fractured porcelain components	125
Figure 4-51	Pre- and post-earthquake circuit breakers and rigid bus connectors	126
Figure 4-52	Braced Hitachi gas circuit breaker	127
Figure 4-53	Power transformers at the Adapazari substation	128
Figure 4-54	Precast reinforced concrete buildings at the Çap textile plant	129
Figure 4-55	Liquid gas tanks at the Habas plant	130
Figure 4-56	Liquid nitrogen tank at the Habas facility	131
Figure 4-57	Collapse of the liquid oxygen tanks	132

Figure 4-58	Buckling of the outer stainless steel shell in a liquid oxygen tank	132
Figure 4-59	Photographs of failed columns beneath a liquid oxygen tank at the Habas facility.....	133
Figure 4-60	Cranes in Mannesmann Boru large-pipe storage area.....	134
Figure 4-61	Damaged port facilities at the SEKA paper mill.....	135
Figure 4-62	Silos at the SEKA paper mill	136
Figure 4-63	Cylindrical liquid gas tanks.....	137
Figure A-1	Typical plan and elevation of the original building	147
Figure A-2	Building damage after the 1967 Akyazi earthquake	148
Figure A-3	Damage in the original building columns in the 1967 Akyazi earthquake	148
Figure A-4	Typical floor plan after retrofit showing the location of new shear walls	149
Figure A-5	Front elevation after the retrofit in 1968 (rigid beams and shear walls added)	149
Figure A-6	City Hall after the November 12, 1999, Duzce earthquake	150
Figure A-7	Acceleration spectra for the August 17, 1999, main shock, the November 11, 1999, aftershock, and the November 12, 1999, main shock	151

LIST OF TABLES

Table 1-1	Recorded peak ground accelerations.....	2
Table 2-1	Key events in the evolution of seismic design codes in Turkey	10
Table 2-2	Values of n_1	13
Table 2-3	Values of n_2	13
Table 2-4	Structural type coefficient, K , from 1975 code	16
Table 2-5	Response modification factors in current seismic codes.....	19
Table 4-1	Industrial facilities visited by the PEER reconnaissance team	78
Table 4-2	Structural damage classification.....	79
Table 4-3	Nonstructural damage classification	79
Table 4-4	Damage to industrial facilities visited by the PEER reconnaissance team	80
Table A-1	Characteristics of the Adapazari City Hall (Anadol 1972)	144

1 Introduction

1.1 1999 Izmit Earthquake

At 3:02 a.m. local time, on August 17, 1999, a M_w 7.4 earthquake occurred on the North Anatolian fault in northwestern Turkey. The hypocenter was located at a depth of 15.9 km at 40.70N, 29.91E, near Izmit, the capital of Kocaeli province, 90 km east of Istanbul. The official death toll was more than 17,225, with approximately 44,000 people injured and thousands left homeless. The majority of deaths and injuries were in the cities of Golcuk, Adapazari, and Yalova (see Figure 1-1). Approximately 77,300 homes and businesses were destroyed, and 244,500 damaged. The total direct cost of the earthquake was estimated to be U.S.\$ 6 billion.

Following the earthquake, the Pacific Earthquake Engineering Research (PEER) Center, which is headquartered at the University of California, Berkeley, sent a reconnaissance team to the epicenter region. The team consisted of Ken Elwood, Khalid Mosalam, Halil Sezen, and Andrew Whittaker of UC Berkeley; John Stanton of the University of Washington; John Wallace of UCLA; and Atila Zekioglu of Ove Arup and Partners, Los Angeles. The team was joined by Jay Love and Chris Smith of Degenkolb Engineers, San Francisco, and Nesrin Basoz of K2 Technologies, San Jose. A geotechnical engineering team supported by PEER and others complemented this team.

1.2 Seismological and Geotechnical Aspects

The 1500-km-long North Anatolian fault, which has many characteristics similar to the San Andreas fault in California, is one of the most extensively studied right-lateral strike-slip faults in the world. During the August 17 earthquake, approximately 110 km of the North Anatolian fault ruptured, with a maximum horizontal offset of 5.5 m (west of Golcuk) and a maximum vertical offset of more than 2.3 m (east of Golcuk). Figure 1-1 shows the measured horizontal and vertical offsets at selected locations. Figure 1-2 is a photograph of the vertical offset near the Ford plant in Golcuk; team member Atila Zeikoglu is standing in front of the ledge formed by the faulting.

The peak ground accelerations recorded in the region affected by the earthquake are shown in Table 1-1. Ground motion data were collected by the Kandilli Observatory and Earthquake Engineering Research Institute of Bogazigi University, and the Earthquake Research Department of the General Directorate of Disaster Affairs. The closest distance to the fault rupture plane and site classifications are also shown in the table. Strong motion stations are listed according to their locations from east to west

An acceleration time history recorded at the Yarimca (YPT) station across the Izmit Bay from Golcuk is shown in Figure 1-3. The secondary shaking evident at 40 sec appears in most acceleration time histories from the Izmit earthquake. However, when these accelerations histories are integrated, this high-frequency shaking has very little effect on the ground velocity and ground displacement. Response spectra for selected acceleration histories for 5% damping are shown in Figure 1-4. (The instrument at Sakarya failed to record the ground motion in the north-south direction.) The spectra have been divided into north-south (Figure 1-4a) and east-west components (Figure 1-4b). Since the fault line runs approximately east-west, these components can be interpreted as approximately fault-normal and fault-parallel, respectively.

Table 1-1 Recorded peak ground accelerations

<i>Station</i>	<i>Distance*</i>	<i>Site class</i>	<i>Peak Acceleration</i>		
			<i>N-S</i>	<i>E-W</i>	<i>Vertical</i>
Duzce (DZC)	14	Soft soil	37	32	36
Sakarya (SKR)	3	Stiff soil	NA	41	26
Izmit (IZT)	8	Rock	17	22	15
Yarimca (YFr)	4	Soft soil	32	23	24
Izmit (IZN)	30	Soft soil	9	13	8
Bursa (BRS)	67	Stiff soil	5	5	3
Arcelik (ARC)	17	Stiff soil	21	13	8
Gebze (GBZ)	17	Stiff soil	26	14	20
Yapi Kredi (YKP)	63	Rock	4	4	3
Istanbul Airport (DHM)	69	Stiff soil	9	8	6
Fatih (FAT)	65	Soft soil	18	16	13
Ambarli (ATS)	79	Soft soil	25	18	8

*Distance from rupture

1.3 Scope and Organization of Report

This report presents information on the development of building and seismic codes in Turkey (Chapter 2), behavior of buildings (Chapter 3), and industrial facilities (Chapter 4) in the epicenter region. The observations presented in the following chapters are those of the PEER reconnaissance team. Because there was minimal damage to bridges during the earthquake, only summary information is presented below. Chapter 5 presents a brief summary and conclusions.

The reconnaissance team documented the collapse of two bridges. Each collapse was a result of fault rupture beneath the piers. Figure 1-5 shows the collapse of the bridge over the Trans-European Motorway. This bridge was composed of four 26-m-long simply supported spans. Each of the spans was positioned on elastomeric bridge bearings. Each span lost the support of at least one end. Figure 1-6 is a view of the bearings and an unseated span from one abutment. Another bridge near Akyazi collapsed (see Figure 1-7), reportedly due to movement of the supporting piers; much of the bridge is submerged in the photograph.

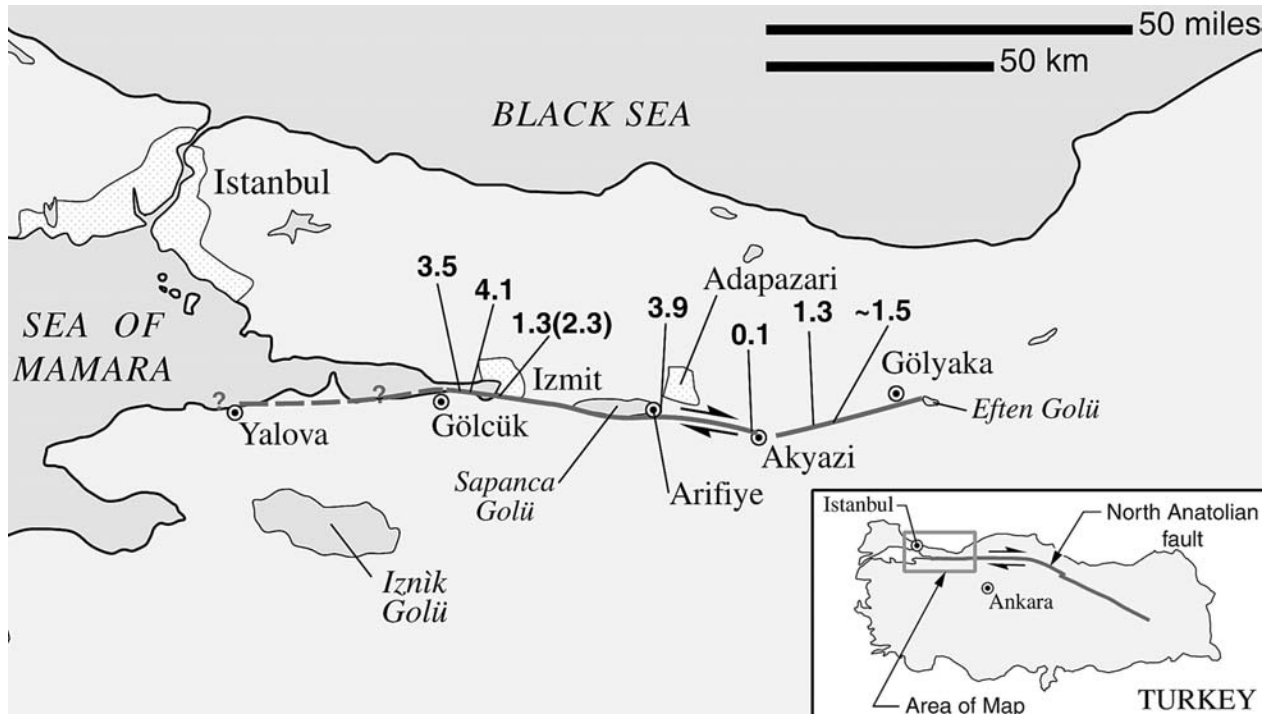
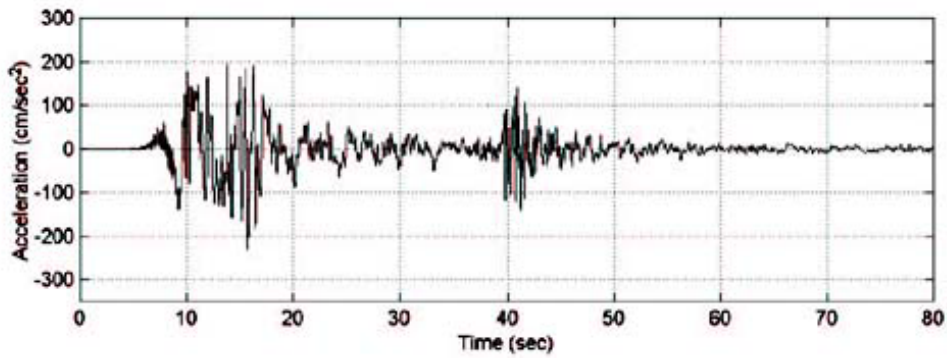


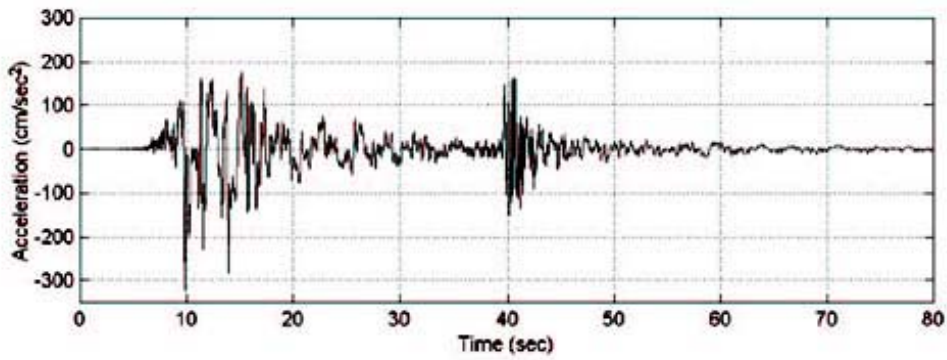
Figure 1-1 Map of affected region showing locations and size (meters) of horizontal offsets and a vertical offset (in parentheses)



Figure 1-2 Vertical offset near Ford Plant in Golcuk

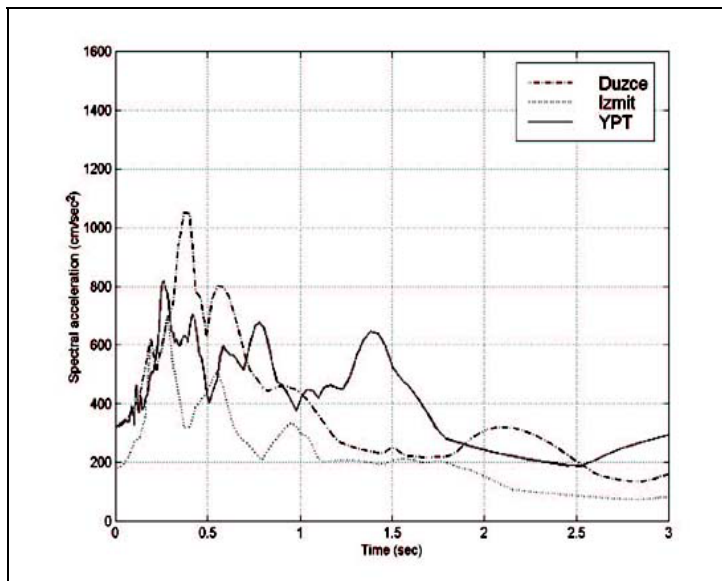


a. east – west component

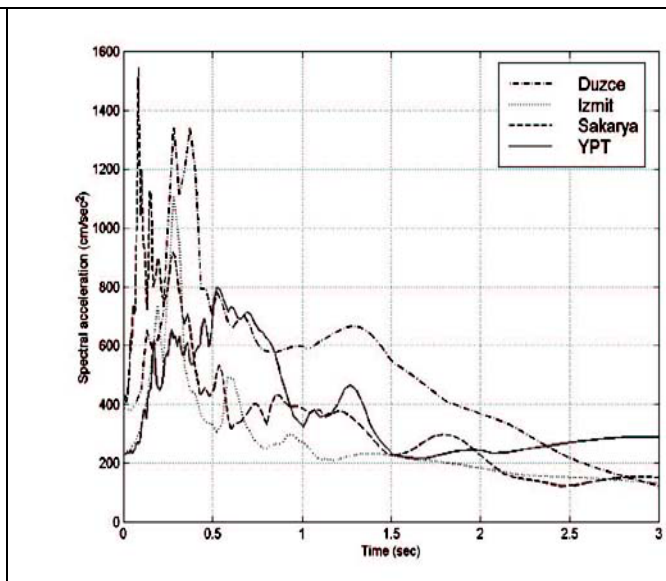


b. north – south component

Figure 1-3 Acceleration time histories from the Yarimca (YPT) Station



a. north – south components



b. east – west components

Figure 1-4 Acceleration Response Spectra for 5% Damping



Figure 1-5 Failure of a bridge over the Trans-European Motorway

Figure 1-6 Unseating of the simply supported span from the abutment-mounted bearings





Figure 1-7 Collapsed and submerged bridge near Akyazi

2 Evolution of Seismic Building Design Practice in Turkey

2.1 Introduction

This chapter describes the practice of seismic design and construction of buildings in Turkey from 1940 to the present. Because reinforced concrete is the most common building material in Turkey, emphasis is placed on reinforced concrete design and construction.

Two codes influence the design and construction of reinforced concrete buildings in Turkey: TS-500, *Building Code Requirements for Reinforced Concrete* (Turkish 1985), termed the “building code” in this report, and *Specification for Structures To Be Built in Disaster Areas* (Ministry of Public Works and Settlement 1975, 1997), termed the “seismic code.”

The building code presents requirements for the proportioning and detailing of reinforced concrete components, and is similar to ACI-318 (ACI 1999) except for the detailing of earthquake effects, which is not covered by the building code. Summary information on the building code is presented in Section 2.3.

Since 1940, the seismic code has included procedures for calculating earthquake loads on buildings. In 1968, restrictions on component sizes and rebar details were introduced for the design of ductile components. Earthquake loads for buildings are calculated using the seismic code similar to U.S. practice in which earthquake loads are calculated using the Uniform Building Code (ICBO 1997). Additional information on the various editions of the code, from 1940 through 1997, is presented in Section 2.4.

The following sections of this chapter present information on major earthquakes in Turkey in the 20th century (Section 2.2), the requirements of the Turkish building code for reinforced concrete (Section 2.3), and Turkish seismic design codes (Section 2.4). A comparison of U.S. and Turkish codes is presented (Section 2.5). Summary remarks are presented in Section 2.6.

2.2 Major Earthquakes in Turkey in the 20th Century

Major earthquakes in Turkey have led to substantial changes in the practice of seismic design and construction. Fifty-seven destructive earthquakes struck Turkey in the 20th century, most occurring along the 1500-km-long North Anatolian fault (see Chapter 1, Figure 1-1). The largest earthquakes on this fault occurred in 1939, 1943, 1944, 1966, 1967, 1992, and 1999 (two earthquakes), resulting in more than 90,000 deaths, 175,000 injuries, and the destruction of 650,000 residential and office buildings.

Table 2-1 lists key events in the evolution of seismic codes in Turkey. Destructive earthquakes have usually resulted in revisions to the codes. In this table and hereafter in this report, "ductile detailing" refers to the use of reinforcement details that provide ductile response in components.

The M7.9 Erzincan earthquake of December 27, 1939, in northeastern Turkey, was the largest earthquake in Turkey in the 20th century. The city of Erzincan was devastated and approximately 32,000 people died. Following that earthquake, the Turkish Ministry of Public Works and Settlement formed a committee to prepare a seismic zone map. The formation of this committee was the first step toward developing regulations for the seismic design of buildings in Turkey.

Table 2-1 Key events in the evolution of seismic design codes in Turkey

<i>Year</i>	<i>Event</i>	<i>Code development</i>
1939	Erzincan earthquake (M7.9)	
1940	Committee formed to develop a seismic zonation map for Turkey	First seismic code published
1942		Earthquake zone map prepared; map promulgated in 1945
1943	Tosya earthquake (M7.2)	
1944	Gerede earthquake (M7.2)	Seismic code revised
1947		Seismic code revised
1949		Seismic code revised
1953		Seismic code revised
1958	Ministry of Reconstruction and Resettlement established	
1961		Seismic code revised
1963		Earthquake zone map revised
1966	Varto earthquake (M7.1)	
1967	Adapazari earthquake (M7.1)	
1968		Seismic code revised
1975		Seismic code revised; ductile detailing introduced
1992	Erzincan earthquake (M6.9)	
1997		Seismic code revised; ductile detailing required
1999	Izmit earthquake (M7.4) Düzce earthquake (M7.2)	

2.3 Building Code Requirements for Reinforced Concrete

The *Building Code Requirements for Reinforced Concrete* provide general proportioning and detailing procedures for reinforced concrete components. Early versions (e.g., 1969) were based on allowable stress design and were similar to other building codes. Major changes were introduced into the code in 1981 and 1985.

The latest version of the building code (1985) permits calculations using both allowable stress design and strength design. For designs in which earthquake loads are considered, stresses for calculations are made using the two following load combinations, U ,

$$U = G + P + E \quad (2-1)$$

$$U = G + 0.9E \quad (2-2)$$

where G is the dead load effect, P is the live load effect, and E is the earthquake effect. Earthquake loads were calculated following the procedures given in the seismic code of the time. However, the building code did not contain any special seismic detailing requirements, and the designer was referred to the seismic code for such information.

2.4 Evolution of Turkish Seismic Design Codes

2.4.1 Years 1940 to 1953

The first seismic design code for buildings was published in 1940, one year after the destructive Erzincan earthquake. The 1940 seismic code was similar to the Italian seismic code of that time (Bayülke 1992; Duyguluer 1997). The base shear, V , was calculated as the product of a lateral force coefficient, C , and the weight of the building, W , namely

$$V = CW \quad (2-3)$$

The value of C was set equal to 0.10 regardless of location. The base shear force was distributed over the height of the building using a uniform load pattern.

An earthquake zonation map for Turkey was prepared in 1942 and promulgated in 1945. The map listed all provinces in Turkey (Duyguluer 1997). Three seismic zones were identified in the map: first degree (hazardous); second degree (less hazardous); and no hazard. No earthquake analysis was required for the no-hazard zone. The interzonal boundaries followed administrative boundaries. According to Duyguluer, the zonation of a province or region was based on the observed or projected intensity of earthquake shaking.

The 1947 code utilized the 1942 maps. The values assigned to C were established on the basis of seismic zone. In first-degree zones, C was set equal to 0.10; in second-degree zones, C was set equal to 0.05. Allowable stresses were increased by 25% for component checking using earthquake load combinations.

In 1949, the zonation map was drawn and appended to the revised code. The coefficients were further reduced to between 0.02 and 0.04 in the first-degree zone, and to between 0.01 and 0.03 in the second-degree zone. The specific value assigned to C was a function of soil and construction type. Duyguluer (1997) noted that the "...proper coefficient was to be established by the design engineer in charge in accordance with the soil formation at the construction site and the constructional characteristics of the building, and approved by the supervising agency." The weight of the building was calculated as

$$W = \sum_i w_i \quad (2-4)$$

and

$$w_i = g_i + np_i \quad (2-5)$$

where w_i is the weight of the floor, g_i is the dead load of the floor, n is a live load coefficient (equal to 0.33 for houses, 0.5 for commercial buildings, and 1.0 for high-occupancy buildings), and p_i is the live load of the floor. Allowable stresses were increased by 50% for component checking using earthquake load combinations, rather than 25% per the 1947 code.

The 1953 code introduced load combinations for earthquake effects. Stresses, U , for earthquake design were calculated using

$$U = G + P + E + 0.5J \quad (2-6)$$

where J is the wind-load effect. No minimum requirements were set for detailing reinforced concrete components.

2.4.2 Years 1954 to 1967

In the 1961 revision of the seismic code, the procedure for calculating the lateral force coefficient, C , was changed to read

$$C = C_0 n_1 n_2 \quad (2-7)$$

where C_0 is a coefficient that varies with building height, and n_1 and n_2 are coefficients that vary with building material, soil conditions, and earthquake zone. Figure 2-1 shows the variation of C_0 with height. For heights greater than 40 m, C_0 was increased by 0.01 for every 3.0 m above 40 m. Tables 2-2 and 2-3 list values for n_1 and n_2 . In Table 2-2, soil type I is “hard and monolithic rock,” soil type II is “sand, gravel, and compact soils...,” and soil type III is “less strong soils other than mentioned” (IAEE 1966).

Table 2-2 Values of n_1

<i>Soil Classification</i>	<i>Building Type</i>	
	<i>Steel</i>	<i>Reinforced Concrete</i>
I	0.6	0.8
II	0.8	0.9
III	1.0	1.0

Table 2-3 Values of n_2

<i>Earthquake zone</i>	n_2
First degree	1.0
Second degree	0.60
Third degree	0.60

In 1963 the earthquake zonation map was substantially revised and the number of zones was increased to four: Zone 1 (first degree), Zone 2 (second degree), Zone 3 (third degree), and Zone 4 (no hazard). The four zones were defined on the basis of the maximum expected shaking using the Modified Mercalli Intensity (MMI) scale. In Zone 1, shaking greater than or equal to MMI VIII was expected; in Zone 2, shaking equal to MMI VII was expected; in Zone 3, shaking equal to MMI VI was expected; and in Zone 4, shaking less than or equal to MMI V was expected. Figure 2-2 is the 1963 earthquake zonation map for Turkey. Because the interzonal boundaries shown in this figure continued to follow administrative boundaries, it was possible to move directly from a first-degree zone (maximum shaking) to a no-hazard or out-of-danger zone (minor shaking).

2.4.3 Years 1968 through 1971

The 1968 seismic code was substantially different from earlier codes. The 1968 code changed the procedures for calculating earthquake demands on building components, introduced requirements for detailing reinforced concrete components, and introduced modern concepts relating to spectral shape and dynamic response. The design base shear of Equation 2-3 was calculated using the weight estimate of Equation 2-5 and a lateral force coefficient, C , that was defined as

$$C = C_0 \alpha \beta \gamma \quad (2-8)$$

where C_0 is a seismic zone coefficient and equal to 0.06, 0.04, and 0.02 for Zones 1, 2, and 3, respectively; α is a soil coefficient equal to 0.80 for rock, 1.00 for sand, gravel, and hard clay, and 1.20 for “...loose soil containing water and poorer soils...”; β is an importance factor equal to 1.50 for critical, high-occupancy, or historically important buildings, and 1.00 otherwise; and γ was a dynamic coefficient, which is calculated as $0.5/T$ for fundamental period, T , greater than 0.5 sec but not less than 0.3, and 1.00 for T less than or equal to 0.5 sec. A coefficient, γ , introduced spectral shape into the Turkish seismic code for the first time. The code wrote that the fundamental period could be calculated as

$$T = 0.09 \frac{H}{\sqrt{D}} \quad (2-9)$$

where H is the height of the building in meters above the foundation, and D is the width of the building in the direction under consideration.

The base shear was distributed over the height of the building using the following equation

$$F_i = V \frac{w_i h_i}{\sum_i w_i h_i} \quad (2-10)$$

where h_i is the height of the floor above the foundation. Equation 2-10 served to replace the uniform load profile of earlier codes with a load profile similar in shape to the typical first mode shape in a building.

Geometry and detailing requirements for reinforced concrete components were also introduced in the 1968 code. Minimum dimensions were specified for beams (150 mm x 300 mm [width times depth]), columns (the smaller of 0.05 times the story height and 240 mm), and shear walls (0.04 times the story height and 200 mm).

The code did not specify minimum spacing for beam stirrups and column ties, but required that “...sufficient transverse reinforcement shall be provided...” and “...where beams frame into columns, the spacing of stirrups and column ties shall be half the spacing at the mid-regions of these members, within a distance not less than the effective depth of the deepest member framing into the joint. Column ties shall be continued within the story beams. ...”

The addendum to the 1968 code included requirements for the use of shear walls. Specifically, the code wrote that if the height of a building exceeded a threshold value (12 m in a first-degree zone, 15 m in a second-degree zone, and 18 m in a third-degree zone), shear walls “...extending along the height of the building shall be provided to transfer lateral earthquake loads to the foundation.”

2.4.4 Years 1972 through 1996

The earthquake zonation map was updated in 1972 and the seismic code was revised in 1975. Key changes to the zonation map included an increase in the number of zones from 4 to 5. Important additions to the seismic code included new methods for calculating earthquake loads on buildings and ductile detailing requirements for reinforced concrete. Information on earthquake effects and analysis, design, and detailing are presented below.

In 1968 the Ministry of Reconstruction and Resettlement embarked on a project to update the earthquake zonation maps based on new information on geologic structure, plate tectonics, historical seismicity, and earthquake occurrence (Duyguluer 1997). Zones were defined on the basis of maximum observed earthquake shaking in the period 1900 through 1970, measured in terms of the Modified Mercalli Intensity, namely, Zone 1 for MMI greater than or equal to IX; Zone 2 for MMI equal to VIII; Zone 3 for MMI equal to VII; Zone 4 for MMI equal to VI, and Zone 5 for MMI less than or equal to V.

The lateral force coefficient of the 1975 code was defined as

$$C = C_o K I S \quad (2-11)$$

where C_o is a seismic zone coefficient and equal to 0.10, 0.08, 0.06, and 0.03, for Zones 1, 2, 3, and 4, respectively; K is a coefficient related to the type of framing system, I is an importance factor (identical to β in the 1968 code), and S is a spectral coefficient. Values of K for different framing systems are presented in Table 2-4. The spectral coefficient was calculated as

$$S = \frac{1}{|0.8 + T - T_o|} \quad (2-12)$$

where T and T_o are the fundamental periods of the building and soil column, respectively. Figure 2-3 presents spectral shapes for soil types I through IV, respectively. Soil types were classified on the basis of blow counts or shear wave velocity, and values for T_o were set for each type. Shear wave velocities for soil types I through IV were set at greater than 700 m/sec for I, 400 to 700 m/sec for II, 200 to 400 m/sec for III, and less than 200 m/sec for IV. The fundamental period was taken as the smaller of the value calculated using Equation 2-9 and

$$0.07N \leq T \leq 0.10N \quad (2-13)$$

where N is the number of stories in the building above the foundation and “... the value of the coefficient ... shall be determined by interpolation between the values of 0.07 and 0.10 according to the degree of general structural flexibility.”

Table 2-4 Structural type coefficient, K , from 1975 code

<i>Structure Type</i>		<i>Filler wall type</i> ¹	<i>K</i>
All building framing systems except as hereafter classified		-	1.00
Buildings with box systems with shear walls		-	1.33
Buildings with frame systems where the frame resists the total lateral force	a. ductile moment-resisting frame	a	0.60
		b	0.80
		c	1.00
	b. nonductile moment-resisting frame	a	1.20
		b	1.50
		c	1.50
Shear wall systems with ductile frames capable of resisting at least 25% of the total lateral force	a	0.80	
	b	1.00	
	c	1.20	

1. Filler wall types: a = reinforced concrete or reinforced masonry walls; b = unreinforced masonry block partition walls; c = light partition walls or prefabricated concrete partition walls

Geometry and detailing requirements for reinforced concrete components were modified in the 1975 code. Minimum dimensions were specified for beams (200 mm x 300 mm [width times depth, = $B \times D$]), columns (the smaller of 0.05 times the story height and 250 mm), and shear walls (0.05 times the story height and 150 mm). Minimum reinforcement ratios and sizes were set for beams (minimum stirrup diameter of 8 mm and minimum stirrup spacing of B or $0.5D$) and shear walls ($\rho = 0.0025, 0.0020$ for horizontal and vertical reinforcement, respectively; maximum rebar spacing of 300 mm or 1.5 times the wall thickness). Figure 2-4 shows sample detailing requirements for beams and shear walls. Minimum floor slab thicknesses were set at 100 mm. Infilled joist slab construction (termed "asmolen" construction) was permitted only in buildings taller than 12 m if shear walls were used as the lateral force-resisting system.

The 1975 code provided much information on minimum details for columns. The minimum rectangular column dimension was limited to 250 mm or 0.05 times the story height; the maximum column width-to-depth ratio was 3.0. The minimum and maximum longitudinal rebar ratios were 0.01 and 0.035, respectively. Columns were divided into three regions as shown in

Figure 2-5: *confinement* regions at each end of the column clear height, a *middle* region, and *beam-column* joint regions. The *confinement* region was defined as the distance not smaller than 0.167 times the column clear height or 450 mm, measured from the slab soffit or beam top surface. The volumetric ratio of transverse reinforcement, ρ , in this region was set at

$$\rho = 0.12 \frac{f_c}{f_y} \quad (2-14)$$

where f_c and f_y are the concrete compressive strength and rebar yield strength, respectively. Hooks of 135° were required on ties in confinement regions; the minimum tie diameter was 8 mm, and the minimum and maximum tie spacings were 50 mm and 100 mm, respectively. In the middle region, tie sizes were based on gravity and earthquake forces (calculated using Equation 2-11). The maximum tie spacing, s_1 in Figure 2-5, was the smaller of 200 mm and 12 times the diameter of the longitudinal rebar.

2.4.5 Years after 1997

The earthquake zonation map was updated (Figure 2-6) and the seismic code revised in 1997. In addition to the equivalent static load method (Equation 2-3), the mode superposition method and linear and nonlinear dynamic analyses were introduced for the seismic design of buildings. The lateral force coefficient was replaced by $A(T)/R_a(T)$, where A is the spectral acceleration coefficient calculated as

$$A(T) = A_0 IS(T) \quad (2-15)$$

The effective ground acceleration coefficient, A_0 , is 0.4, 0.3, 0.2, and 0.1 for the first four seismic zones, respectively. Note that the fifth seismic zone was specified to have no earthquake hazard. The importance factor, I , is 1.0 for ordinary structures and varies between 1.0 and 1.5. The spectrum coefficient, S , which defines the design acceleration spectrum, is given by three equations in the short-period, constant-acceleration, and constant-velocity ranges, respectively. These ranges are delineated by spectrum characteristic periods, T_A and T_B , which vary as a function of soil type. The maximum spectral amplification is 2.5. The seismic load reduction factor in this code is similar to the response modification factor in U.S. codes, except that the seismic load reduction factor reduces linearly from the maximum value of R , which is tabulated in the code, to 1.5 at zero period. The value of R depends on the assumed ductility (high or normal) of the system and varies between 3 and 8.

Reinforced concrete buildings are classified as systems of either high or nominal ductility based on the detailing of the components. Detailing requirements are more stringent for systems with high ductility. Transverse reinforcement requirements for beams are presented in Figure 2-7. These requirements apply for frames of both high and nominal ductility.

The detailing requirements for columns of high and nominal ductility levels are most similar. The minimum cross-section dimensions are 250 mm by 300 mm. Information on the transverse reinforcement requirements along the height of a column are shown in Figure 2-8. All hoops must have 135° seismic hooks at both ends. Cross ties may have 90° hooks at one end. The sum of the column strengths at a beam-column joint must exceed 120% of the sum of the beam strengths at that joint. The shear strength of a column must exceed the shear force associated with the plastic moments in the column. The only major provision that is not applicable for columns of nominal ductility level is the spacing of transverse reinforcement along the confinement zones (Figure 2-8), which is required to be half the spacing in the column middle region. Lap splices of column longitudinal rebar should be made in the middle third of the column. If column rebar are spliced at the bottom of a column, the splice length is increased to 125% or 150% of the development length of the bar in tension, depending on the number of bars being spliced. For columns in frames of nominal ductility, the maximum spacing of the transverse reinforcement between the confinement zones is increased by a factor of 2 over the spacing shown in Figure 2-8. For shear walls, the minimum wall thickness is the smaller of 0.067 times the story height and 200 mm.

2.5 Comparison of United States and Turkish Codes of Practice

Figure 2-9 presents 5% damped linear elastic acceleration response spectra for rock and soft soil sites calculated using the provisions of the 1997 *Uniform Building Code* (ICBO 1997) and the 1997 *Turkish Specification for Structures To Be Built in Disaster Areas* (Ministry 1997) for the regions of highest seismicity in each country. The Uniform Building Code (UBC) spectra shown in this figure do not include near-field amplification factors, N_a and N_v , that must be applied if the site of the building is within 15 km of a major active fault. Putting these factors aside, the spectral demands of the two current codes are very similar.

Figure 2-10 presents the lateral force coefficient spectra (C in Equation 2-3) for the 1975 and 1997 Turkish codes and the 1997 UBC for reinforced concrete moment-resisting frames on rock and soft soil sites. Such frames were chosen for the purpose of comparison because reinforced concrete moment-resisting frames are the most common seismic framing system in Turkey for building construction. To construct the "allowable-stress-design" spectra for the 1975 Turkish code, K was taken as 0.80 and 1.50 for ductile and nonductile reinforced concrete moment frames, respectively; C_0 was set equal to 0.10. The ordinates were then increased by 40% to construct "strength-design" spectra to facilitate comparison with the 1997 Turkish seismic code and the 1997 UBC. To construct the spectra for the 1997 Turkish code, A_0 and the importance factors were set equal to 0.40 and 1.0, respectively, and R was set equal to 4 and 8 for reinforced concrete moment-resisting frames of nominal and high ductility, respectively. To construct the spectra for the 1997 UBC, soil types S_B and S_E were assumed for the rock and soft soil sites, respectively; near-field factors were not considered; the importance factor was set equal to 1.0, and R was set equal to 3.5 and 8.5 for ordinary moment-resisting frames (OMRF) and special moment-resisting frames (SMRF), respectively. (The OMRF and SMRF of the UBC correspond approximately to frames of nominal and high ductility in the Turkish code, respectively.)

For modern reinforced concrete moment-resisting frames of high ductility (the SMRF in the U.S.), the ordinates of the 1997 Turkish lateral-force-coefficient spectra exceed those of the 1997 UBC for both rock and firm soil sites. Recognizing that the prescriptive details of the 1997 UBC and the 1997 Turkish code for frames of high ductility are similar, the performance of buildings designed to either code should be similar if the standards of construction are comparable.

Table 2-5 presents values of R in the 1997 UBC and the 1997 Turkish codes for different framing systems. These values are similar for each type of framing system. Further review of the two codes indicates similarities in most other regards. Because the linear-elastic acceleration response spectra (Figure 2-9) are similar in both codes for the regions of highest seismicity, buildings designed and constructed in accordance with these two codes should perform equally if the construction quality is similar.

Table 2-5 Response modification factors in current seismic codes

<i>Lateral force-resisting system</i>	<i>Country</i>	
	<i>1997 Turkey^{1,2}</i>	<i>1997 USA²</i>
Reinforced concrete shear wall	6	5.5
Reinforced concrete moment-resisting frame	8	8.5
Steel eccentrically braced frame	7	7
Steel moment-resisting frame	8	8.5

1. Framing systems of high ductility
2. 1997 codes in Turkey and USA

2.6 Summary Remarks

Revisions to the practice of earthquake engineering in Turkey have generally followed major, damaging earthquakes. This trend is not unique to Turkey because changes in design practice in Japan, Mexico, and the United States have followed major earthquakes in those countries.

Provisions for special detailing of reinforced concrete moment-resisting frames for ductile response were introduced in Turkey in 1975. Such requirements were similar to those introduced in the United States in the early 1970s. However, the construction of buildings with ductile details was not mandated as it was in California in the 1970s. Rather, buildings could be constructed without special details for ductile response (frames of nominal ductility) or ductile details (frames of high ductility). Because it was cheaper to construct stronger buildings without special details for ductile response (nonductile detailing) than weaker buildings with ductile detailing, nonductile moment-resisting frame construction was most prevalent in Turkey up to the time of the Izmit earthquake.

The current codes of practice in Turkey and the United States are similar in terms of strength and detailing requirements. However, two key changes to the Turkish *Specification for Structures To Be Built in Disaster Areas* are recommended:

1. A factor that accounts for the close proximity of a structure to a fault (i.e., a near-field factor) should be included in the design force equation.
2. Special details for ductile component response and the use of rules for ductile system response should be mandatory in moderate and severe seismic zones, regardless of the lateral forces used for design.

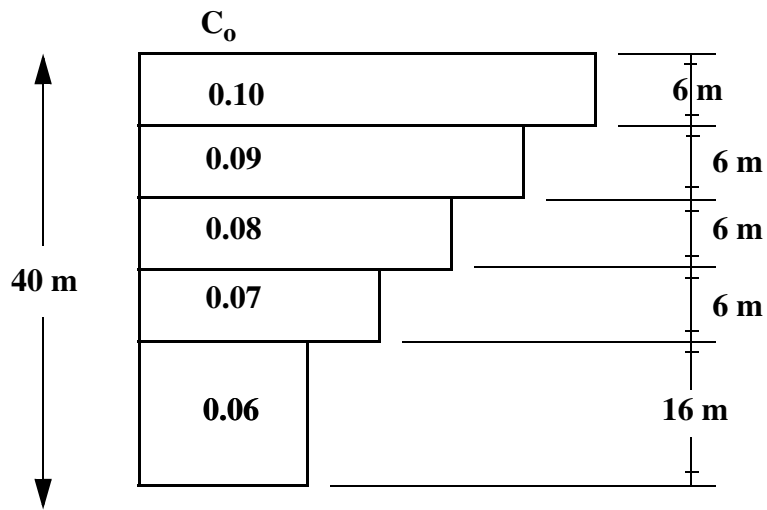


Figure 2-1 Distribution of coefficient C_0 with height above grade in 1961 seismic code

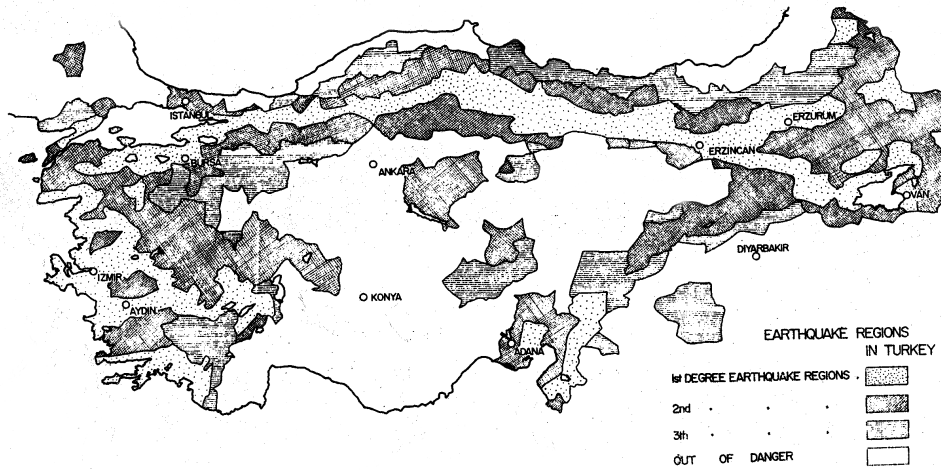


Figure 2-2 1963 earthquake zonation map (IAEE 1966)

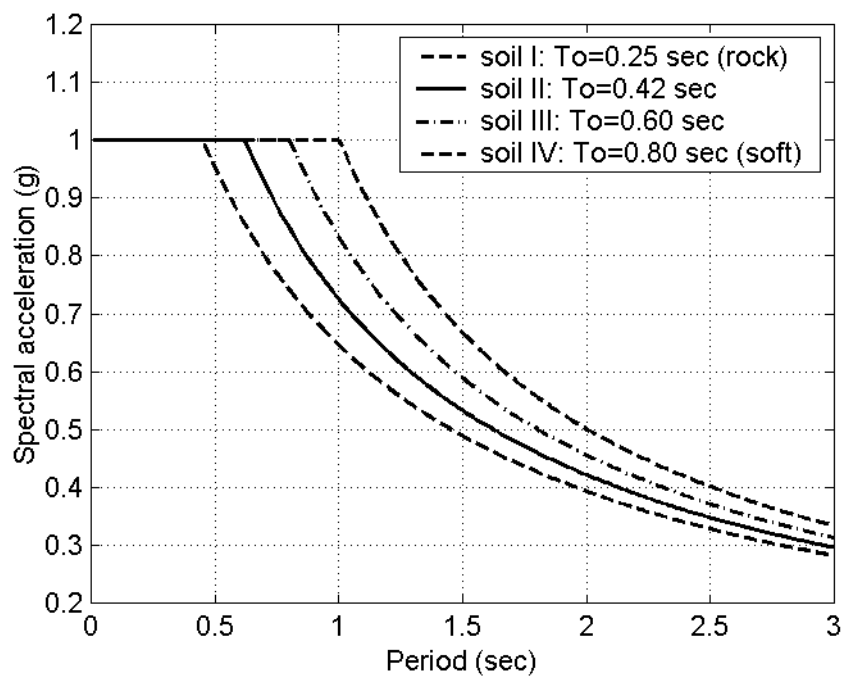


Figure 2-3 Spectral coefficients, S , from 1975 seismic code

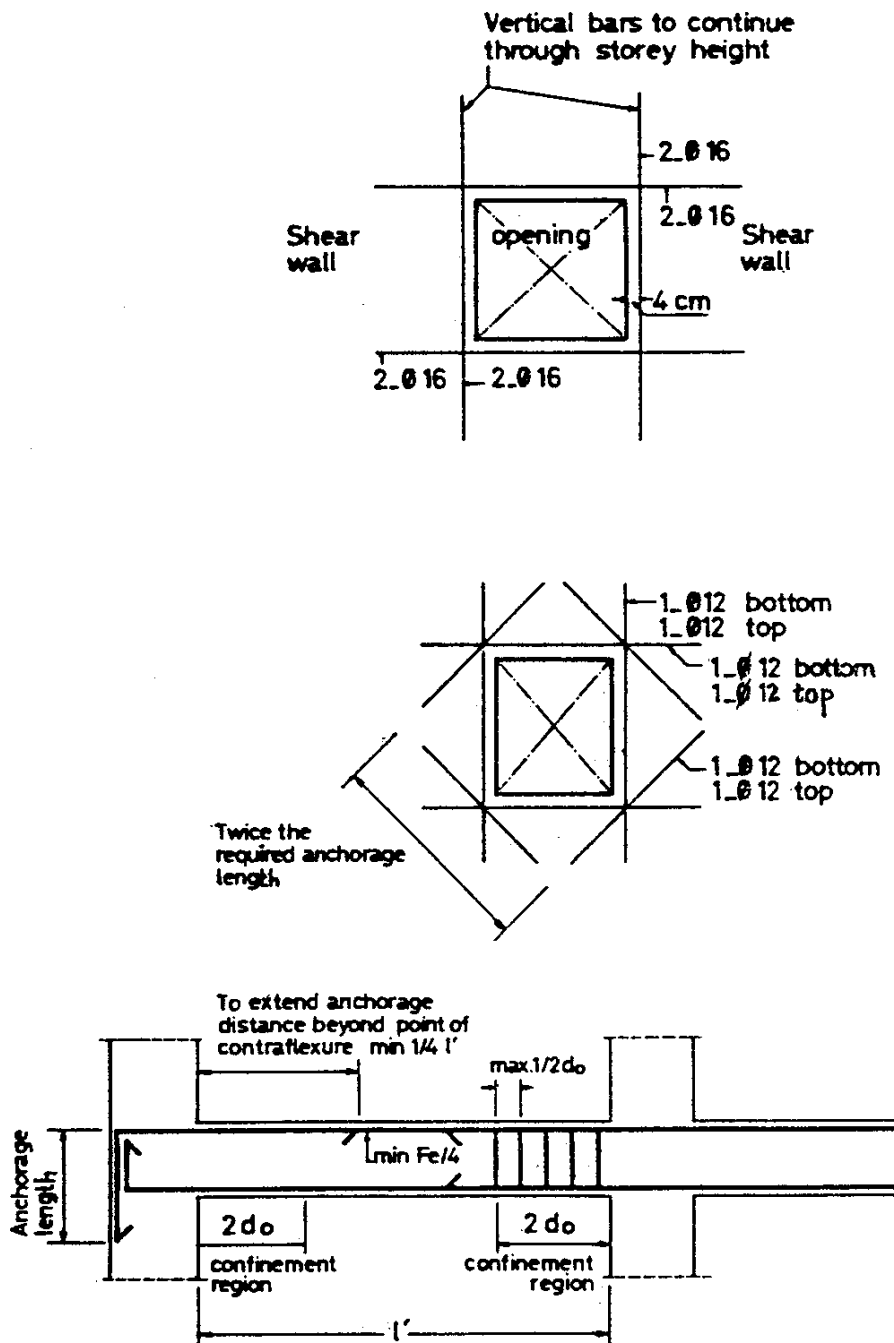


Figure 2-4 Detailing requirements for beams and shear walls from 1975 seismic code

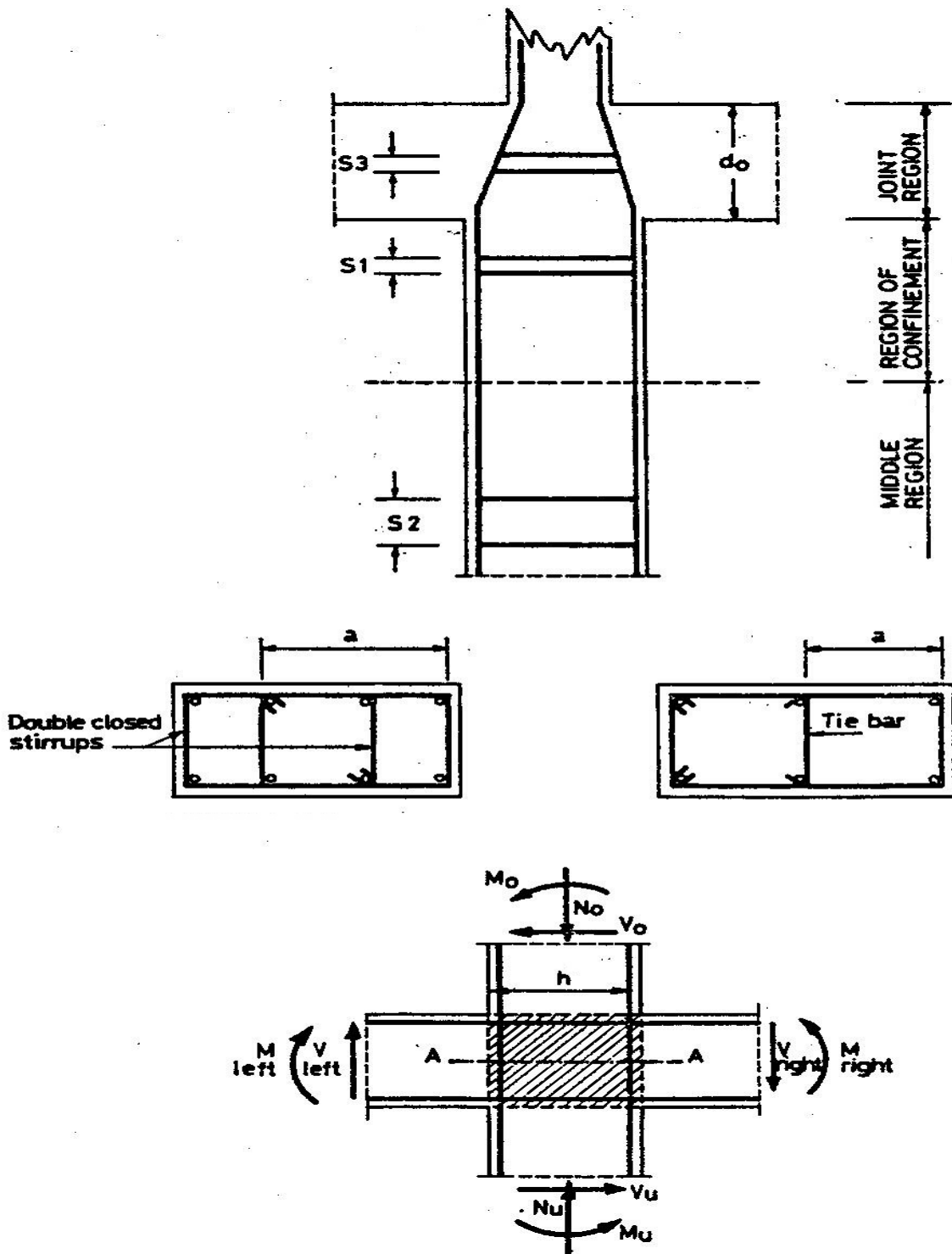


Figure 2-5 Detailing requirements for columns from 1975 seismic code

EARTHQUAKE ZONING MAP FOR TURKEY

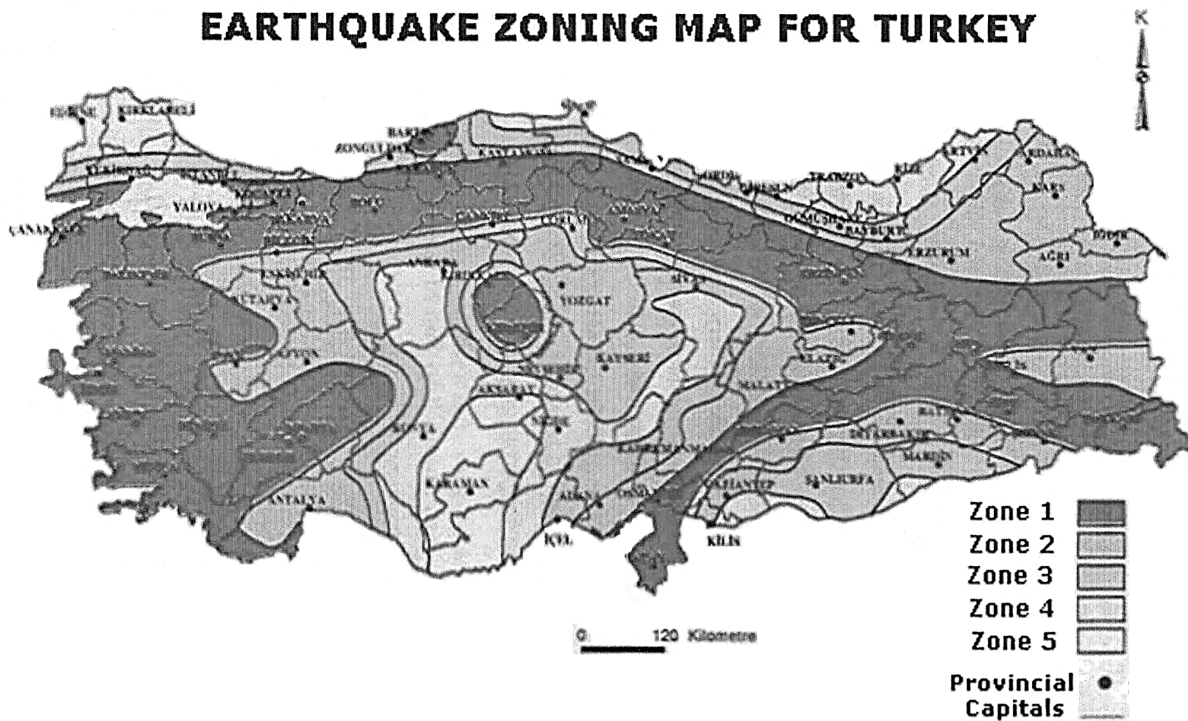


Figure 2-6 Earthquake zonation map of Turkey in the 1997 seismic code

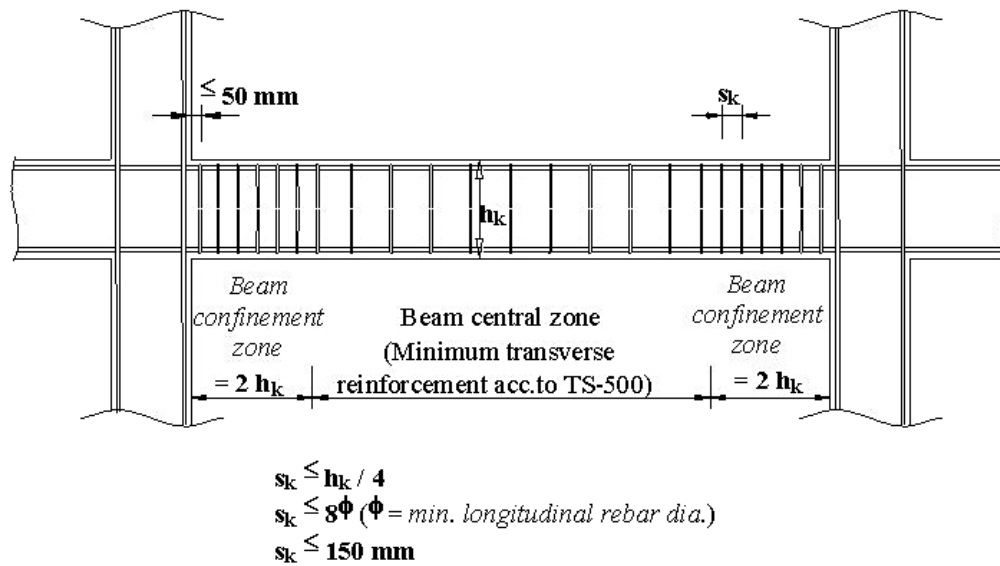


Figure 2-7 Transverse reinforcement requirements for beams in the 1997 seismic code

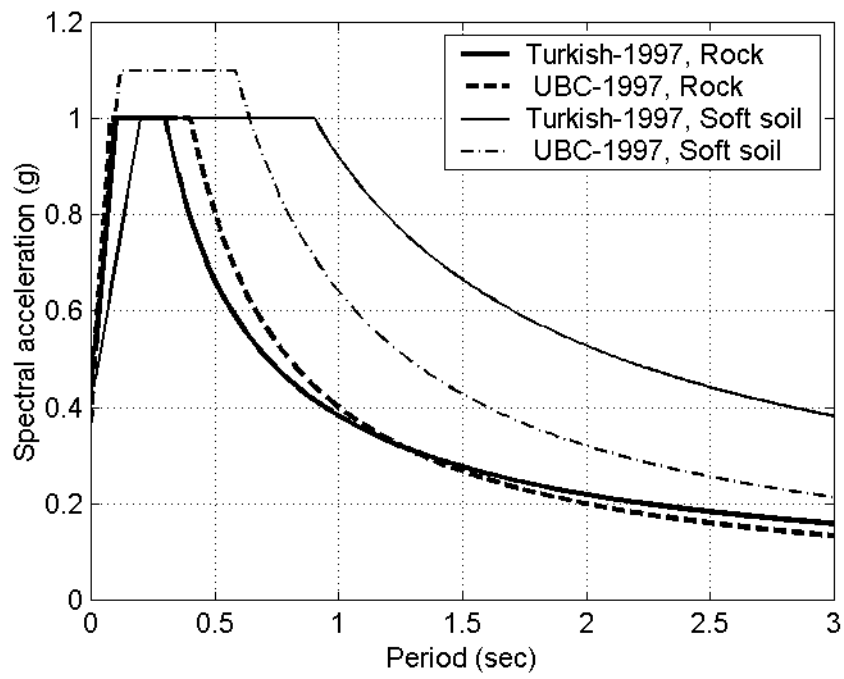
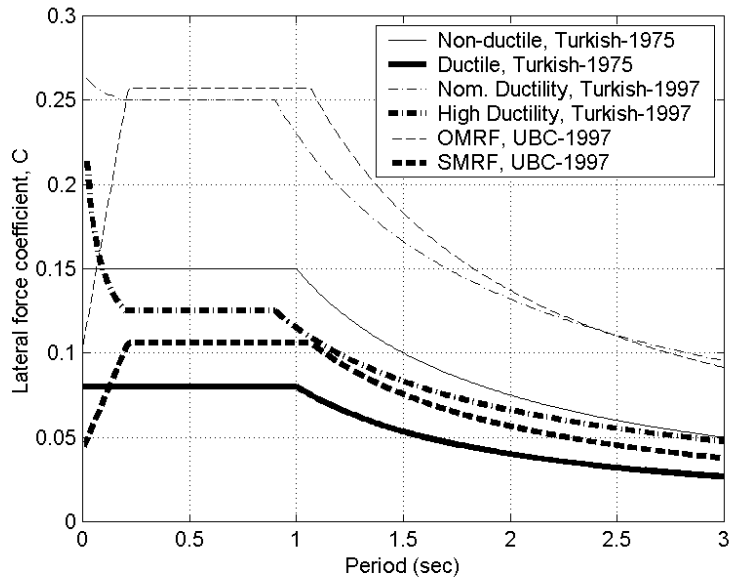
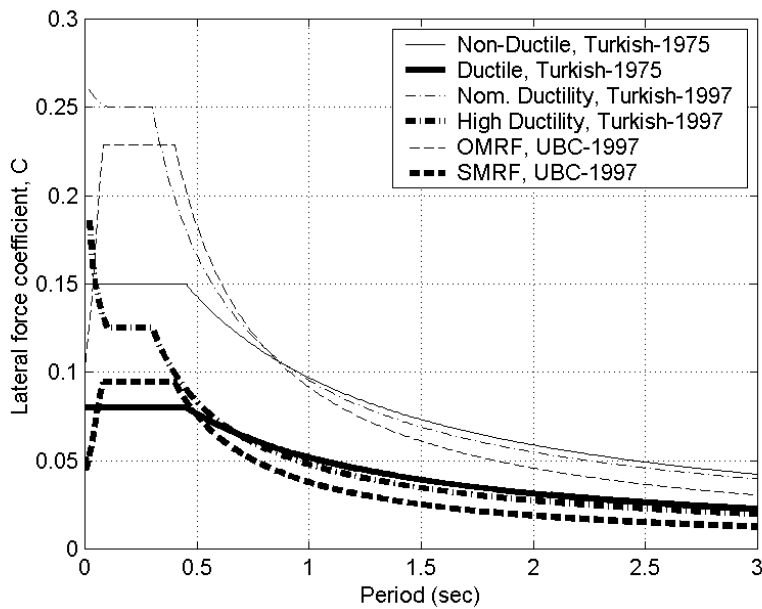


Figure 2-9 Comparison of elastic response spectra from the 1997 UBC and the Turkish seismic codes



a. soft soil sites



b. rock sites

Figure 2-10 Comparison of lateral force coefficient, C , in the 1997 UBC, and 1975 and 1997 Turkish seismic codes

3 Reinforced Concrete Frame and Wall Buildings

3.1 Introduction

One of the missions of the Pacific Earthquake Engineering Research (PEER) Center is to develop procedures and guidelines for performance-based earthquake engineering. The damage resulting from the Izmit earthquake gave the reconnaissance team a unique opportunity to study response limit states for selected buildings impacted by the earthquake. This chapter summarizes the key observations of the reconnaissance team regarding residential and commercial reinforced concrete construction in Turkey. Construction practices are described and the responses of moment-resisting frames and the behavior of shear walls are summarized. In the epicentral region, the two most widely used framing systems for residential and commercial construction are reinforced concrete moment-resisting frames and shear walls, and most of the loss of life and damage in the Izmit earthquake was a result of the poor performance of reinforced concrete buildings.

3.2 Construction Practice

The quality of the construction of residential and commercial buildings in the epicentral region varied widely. Both individuals and registered contractors undertake building construction work. Commercial construction is typically built by registered contractors and was generally of better quality than residential construction. Anecdotal evidence suggests that the level of inspection by regulatory officials of building construction work undertaken by registered contractors and individuals was limited prior to the earthquake.

The reconnaissance team found evidence of both extremely good and extremely poor commercial construction. One example of excellent quality construction is the building of Figure 3-1 that was located in central Yalova. Residential construction quality also ranged from excellent to poor. Although construction work by registered contractors was generally of better quality than that by individuals and homeowners, the quality of contractor-completed construction was often poor by U.S.



Figure 3-1 High quality apartment construction, Yalova

standards. Figure 3-2 shows a completed shear wall in a multistory apartment building in Yalova. The vertical and horizontal rebar in the shear wall can be seen on the exterior face of the wall. Although buildings in Yalova suffered damage in the earthquake, the apartment building was not damaged despite the poor quality of the concrete evident in the photograph.

An example of residential apartment construction by a homeowner in a village outside of Gölcük is shown in Figure 3-3. The shoring is composed of cut and trimmed tree limbs. (In most instances, conventional steel and timber shoring is used for apartment construction over four stories.) Timber planks are used to form columns, beams, and slabs. Photographs of the second floor of the apartment building are presented in Figure 3-4. Slabs typically span in one-direction and are approximately 100 mm in thickness. Beams span 2 m to 4 m, range in depth up to 500 mm, and are typically 200 mm wide. Bent-up rebar can be seen in Figure 3-4. Transverse ties with 90° hooks are used. The beam rebar details are nonductile. Blade columns (long and narrow in plan) are routinely used in apartment buildings to

enable the builder to construct the columns within the thickness of the wall. Some column details can be seen in Figure 3-4. Vertical rebar are spliced at the floor level. Typical splice lengths are approximately 1 m and no additional ties are provided in the splice region. Transverse reinforcement with 90° degree hooks is typical. Joint shear reinforcement is not provided. The column rebar details are nonductile.



Figure 3-2 Poor quality construction of a shear wall in an apartment building in Yalova



Figure 3-3 Homeowner apartment building construction

Smooth rebar is commonly used for reinforced concrete construction in the epicentral region. The yield strength of such rebar is approximately 275 MPa. Smooth rebar is used because it is less expensive and more readily available than deformed rebar, and is also easier to bend and cut on site. The strength and quality of the concrete varied widely as noted above. Concrete is typically batched on site for low-rise residential and commercial construction, and standard quality control procedures such as slump tests are rarely used. Low-strength concrete was identified in a number of damaged buildings visited by the reconnaissance team. Some samples were weak enough to crush by hand.

The reconnaissance team was surprised by the volume and type of residential construction. Specifically, there was much unoccupied new residential construction, and there were many incomplete single- and two-story additions to existing construction. Local experts explained that homeowners often added stories to existing apartments or constructed new multistory apartments as a hedge against inflation. The quality of such construction was often poor; it is highly likely that much of this construction was neither engineered nor approved by the local jurisdiction.



Figure 3-4 Typical gravity framing including beam and column details

3.3 Moment-Resisting Frame Construction

3.3.1 Typical Framing Systems for Residential Construction

Residential buildings in the epicentral region typically range in height between two and seven stories. Sample two- and four-story buildings are shown in Figures 3-5a and 3-5b, respectively. Because federal agencies limit the building first-story footprint-to-plot ratio, cantilever construction in the form of beams or as masonry floor framing (see Section 3.3.2) is often employed at the second-floor level to maximize the gross floor area of the building. Cantilever construction can be seen in both buildings of Figure 3-5.

Figure 3-6 presents photographs of a three-story building that was under construction at the time of the earthquake. A plan of the second-floor framing is shown in Figure 3-7. The column and beam orientation shown in Figure 3-7 suggests that the framing system is much stiffer and stronger in the direction perpendicular to the street (parallel to the y -axis of Figure 3-7), assuming that similar rebar are used in all beams and columns in this building. The ratio of total column area to plan footprint in this building is 1.3%.



a. Two-story building



b. Four-story building

Figure 3-5 Typical framing systems in epicenter region

A plan of the roof framing of a five-story moment-resisting frame building is shown in Figure 3-8. The column orientations and locations are such that there are no moment-resisting frames of more than one bay in either direction of the building in the fifth story. Such framing likely possesses limited strength and stiffness that, if coupled with nonductile reinforcement details, results in a vulnerable building in the event of earthquake shaking.



a. north-south elevation

Figure 3-6 Three-story moment-resisting frame east of Gölcük



b. east-west elevation showing fault rupture

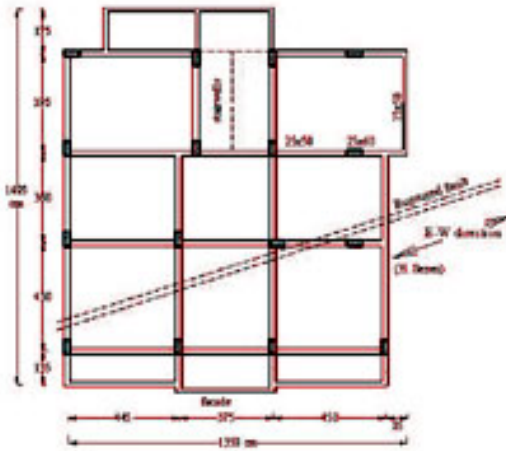


Figure 3-7 Floor plan for the three-story building shown in Figure 3-6

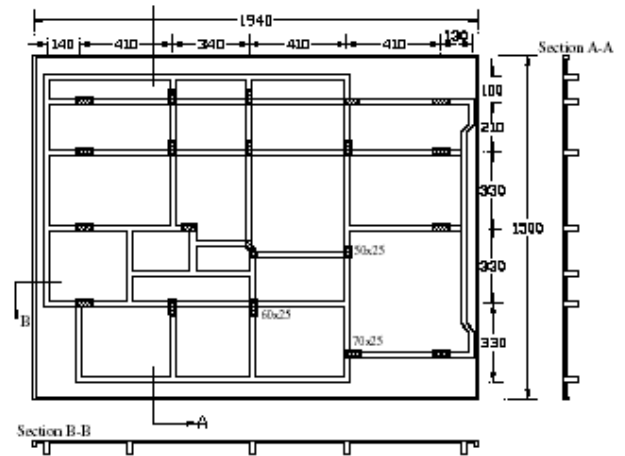


Figure 3-8 Plan of roof framing for a five story apartment

3.3.2 Typical Construction Details

Many apartment buildings in the epicentral region are constructed with a tall first story for commercial (shop) occupancy. Typical story heights range between 3.5 to 4.5 m in the first story and 2.8 to 3.0 m in the upper stories. Most columns in such construction are blade columns with an aspect ratio of approximately 3. Column plan dimensions range between 150 mm x 500 mm to 250 mm x 800 mm. The longitudinal rebar ratio ranges between 1% and 2%; 12 to 16 mm diameter smooth rebar are generally used. Transverse ties are smooth rebar of 6 to 10 mm diameter with 90° hooks. The spacing of transverse ties is typically 200 to 250 mm along the clear height of the column.

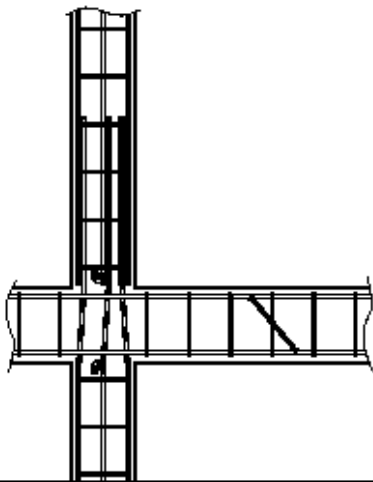


Figure 3-9 Typical modern beam and column rebar details

Typical beam spans ranged between 3 and 5 m. Beam depths and widths ranged between 200 to 250 mm and 500 mm to 600 mm, respectively. Transverse ties are smooth rebar of 6 to 10 mm diameter with 90° hooks. The spacing of transverse ties is typically 200 to 250 mm along the clear length of the beam. Bent-up longitudinal rebar, often used for reasons of economy to provide shear resistance to gravity loads and to increase negative moment resistance for gravity loads at supports, do not resist shear force if the loads are reversed due to earthquake shaking.

Information on column and beam rebar details is provided in Figure 3-9. Corner column rebar are spliced above the floor slab with lap lengths of 40 to 70 bar diameters. Side-face column rebar are either spliced per corner rebar or terminated above and below the joint with 180° hooks. No transverse reinforcement for the purpose of confinement is provided in the hinge, joint, or splice regions. Bent-up beam rebar is shown in the typical section.



Figure 3-10 Hollow clay tile block used for infills

Interior and exterior infill walls are constructed of either *hollow clay tile* or lightweight gas-concrete blocks. The hollow clay tile block is more widely used than the gas-concrete block and is extremely brittle. The block infill is not reinforced nor is it anchored to the structural framing with masonry ties. Block infill walls are built in contact with the structural framing and add significant stiffness and strength to the framing system. Photographs of hollow clay tile block are shown in Figure 3-10.

Common slab systems include the one-way and *asmolen* slabs. One-way slabs range in thickness from 80 mm to 120 mm, and span distances up to 4 m. For longer spans and heavy loadings, the one-way, or *asmolen*, joist system is typically used. This system is composed of one-way joists that are formed by hollow clay tile blocks; the slab between the joists is cast directly atop the blocks. The thickness of the *asmolen* slab is usually 300 mm (200 mm block and 100 mm slab) or 320 mm (250 mm block and 70 mm slab). Figure 3-11 shows the underside of three *asmolen* floor systems.



Figure 3-11 Asmolen floor system in a four-story building

3.4 Behavior of Moment-Resisting Frame Construction

Moment-resisting frame construction fared poorly during the Izmit earthquake. According to official estimates, more than 20,000 moment-frame buildings collapsed, and many more suffered moderate to severe damage. Three- to seven-story apartment buildings were hard hit, although many had been constructed in the past 20 years. Many of the collapses are attributed to the formation of soft

first stories that formed as a result of differences in framing and infill wall geometry between the first and second stories, the use of nonductile details, and poor quality construction.

Figure 3-12 shows the collapse of six moment-resisting frame buildings in a village on the outskirts of Gölcük. Every moment-resisting frame building on this street collapsed, and 122 people died in these buildings. Nonductile details were observed in every (collapsed) moment-frame building on this street.



Figure 3-12 Collapse of moment frame buildings, Gölcük



Figure 3-13 Collapse of moment-frame and wall buildings, Adapazari

Similar collapses were common in the epicentral region. Figure 3-13 shows the extent of the destruction in Adapazari, a major city approximately 10 km from the line of rupture. Many of these buildings were constructed with hollow clay tile infill in the frames perpendicular to the sidewalk. Because the buildings often housed shops and commercial space in the first-story, glass panels and not hollow clay tile infill walls were placed between the first story columns adjacent to the sidewalk, but tile infill was used in the upper stories. Such an arrangement of tile infill created stiffness discontinuities in these buildings, which may have contributed to their collapse.

3.4.1 Moment-Frame Buildings Straddling or Adjacent to Line of Rupture

Not all moment-frame buildings that straddled the line of rupture collapsed. The fault ran directly beneath the building shown in Figure 3-6, but this building suffered only modest damage despite approximately 1 m of horizontal offset beneath the foundation. The lack of damage can be attributed to the stiffness of the building's 1-m-deep raft foundation. Three hundred meters from the building of Figure 3-6, a moment-frame school building that straddled the fault collapsed completely (Figure 3-14). Figure 3-15 shows collapsed and damaged moment-frame buildings on the Gölcük naval base. The horizontal offset of the fault beneath these buildings was on the order of 4 m. Fault rupture beneath a five-story building (Figure 3-16) located approximately 200 m east of the naval base caused a partial collapse.



Figure 3-14 Collapsed school building that straddled the line of rupture



Figure 3-15 Collapsed and damaged moment-frame buildings on the Gölcük navy base



a. Collapsed building



b. View of failed first story

Figure 3-16 Collapsed building that straddled the line of rupture

“Near-field” is the common term used to define the zone within 5 to 10 km of a major fault. Earthquake shaking in the near field is often severe, as illustrated by recorded ground motions obtained from the Northridge (1994) and Kobe (1995) earthquakes. Widespread collapse of older construction is to be expected in the near field due to the intensity of the earthquake shaking. Although many moment-frame buildings in the near field of the Izmit earthquake suffered gross damage or collapsed, some fared surprisingly well. Shown in Figure 3-17, the four-story moment-frame building is sited within 2 m of the line of rupture and yet suffered no visible damage despite 1.2 m of horizontal offset and 2.35 m of vertical offset on the fault. Figure 1-2 shows another view of the same building. The reasons for such good performance of this 10- to 30-year-old frame building with masonry infill are unknown.



Figure 3-17 Undamaged building located within 2 m of the line of rupture

3.4.2 Variability of Moment-Frame Building Response

Figure 3-18 is a photograph of two six-story nonductile moment-frame buildings in Gölcük. One of the buildings collapsed completely, whereas the building immediately adjacent suffered only superficial damage in the form of minor cracking in the first-story columns. Much of the first story of the collapsed building was intact. Careful examination of the first stories in both buildings showed that the buildings had similar plan footprints and common construction details. It is likely that the two buildings were nearly identical and that the same contractor constructed both buildings. Both buildings were probably subjected to similar levels of earthquake shaking, yet one building remained in the elastic range and performed well, while the other collapsed. This raises many questions regarding limit states for nonductile moment-frames. Small differences in the strength of these nonductile buildings caused by the use of different construction materials and different construction practices and workmanship could account for the substantial difference in performance.



a. lightly damaged six-story building



b. collapsed six-story building

Figure 3-18 Variability of building response

3.4.3 Role of Infill Walls in Response of Moment-Frame Buildings

Hollow clay tile and gas-concrete masonry infill walls are widely used in the epicentral region. As noted in Section 3.3.2, these walls are unreinforced and nonductile. The walls abut the frame columns but are not tied to the frame. The high in-plane stiffness of the masonry infill that is developed by diagonal strut action can dictate the response of the more flexible moment-resisting frame. Figures 3-19a and 3-19b show complete and partial damage to hollow clay tile walls in four- and thirteen-story buildings, respectively. The four-story building was under construction at the time of the earthquake; the thirteen-story building was constructed in the early 1970s.



a. four-story building



b. thirteen-story building

Figure 3-19 Varying degrees of damage to infill masonry walls

Damage to infill masonry walls was concentrated in the lower stories of buildings because of higher demands on the strength of the moment-frame-infill wall system. Figure 3-20 illustrates the distribution of damage to infill walls in two buildings, one near Gölcük, and one in Degirmendere. In these buildings, the lateral stiffness of the masonry infill walls is likely of the same order or greater than that of the moment-frames. For these buildings not to collapse following the failure of the infill walls the moment-frames must have possessed significant strength and some limited ductility.



a. infill wall damage in Gölcük



b. infill wall damage in Degirmendere

Figure 3-20 Damage to infill masonry walls

Figure 3-21 shows two views of a collapsed apartment building in Gölcük. The first two stories of this building failed completely but damage in the upper three stories was limited. The long infill walls in the upper three stories have significant elastic strength and stiffness—probably much greater stiffness and strength than the moment-resisting frame. If the infill walls in the upper three stories of the building are indicative of the infill in the failed stories, the first- and second-story infill walls likely played an important role in the collapse of the building. The brittle fracture of the first- and second-story infill masonry walls would have overloaded the nonductile first- and second-story frame columns, resulting in a complete failure.



a. view of front face of building



b. view of infill wall perpendicular to sidewalk

Figure 3-21 Collapsed apartment building in Gölcük

The first two stories of the building in Figure 3-22 collapsed. The infill masonry walls and moment-frame construction in the third and fourth stories (first and second stories of the collapsed building) suffered major damage. Damage in this building reduced with increased height above the sidewalk. Failure of the infill masonry in the first and second stories of the building likely precipitated the collapse of the building.

Irregular placement of infill masonry walls can produce discontinuities of stiffness in moment-frame buildings. Consider the building in which the moment-frame is both flexible and weak by comparison with the upper stories (Figure 3-23). In the first story of this building, infill masonry walls are present in the back face of the building and in the two faces perpendicular to the sidewalk. The front of the building was open in the first story. The lateral stiffness of the building was likely large in the direction perpendicular to the sidewalk and much smaller parallel to the sidewalk. Deformation is concentrated in the first story of this building, parallel to the sidewalk, due to the weakness and flexibility of the moment-frame and the lack of infill masonry in the front of the building. The first-story columns in this building were badly damaged and likely close to failure.



Figure 3-22 Failure of two stories of moment-frame building with infill masonry

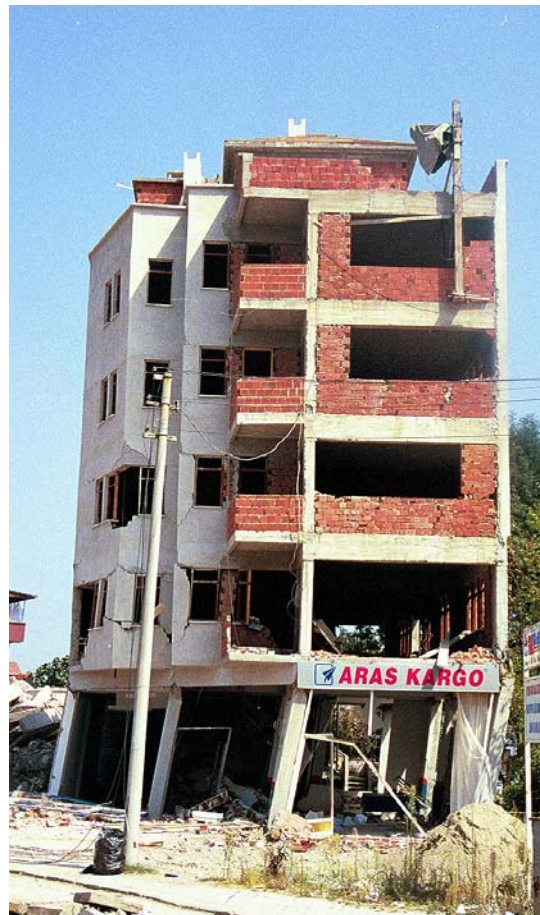


Figure 3-23 Formation of a soft and weak story

3.5 Response of Moment-Frame Components

Previous sections of this discussion on moment-frame construction have focused on the response of moment-frame systems. This section of the report addresses the response of the components of moment-frames, namely, beams, columns, beam-column joints, and slabs.

3.5.1 Beams

The reconnaissance team observed little damage to interior moment-frame beams because columns were generally weaker than beams. One type of beam damage is shown in Figure 3-24. The building in this figure suffered a partial story collapse because the fault ruptured beneath the building. The beams shown in the frame elevation were forced to accommodate the partial collapse and were badly damaged at the beam-column connection due to slip of the smooth longitudinal beam rebar. In many cases, beam bottom rebar was inadequately anchored in and through beam-column joints.



Figure 3-24 Damage to a nonductile reinforced concrete beam



Figure 3-25 Failure of lap splices in a moment frame connection

3.5.2 Columns

The majority of moment-frame component failures were in columns and were due to (a) the use of nonductile details and unconfined lap splices, (b) excessive beam strength, and (c) interaction between the columns and the infill masonry walls.

Lap splices in moment-frame columns were typically made immediately above the floor framing or the foundation. The photograph of the exposed lap splice of Figure 3-25 is from a moment-

frame building in Adapazari. The lap splices in this column were approximately 35 bar diameters in length and were located in a plastic hinge zone. Widely spaced transverse ties with 90° hooks were used in this column; no cross ties were present. The 90° hooks on the ties opened during the earthquake, and the limited strength and confinement afforded by the ties were lost.



Figure 3 –26 Typical transverse reinforcement details in columns
a. view of damaged blade column
b. transverse tie details in blade column

Shear reinforcement was lacking in most damaged columns observed by the reconnaissance teams. The transverse tie details of Figures 3-26, 3-27, and 3-28 were common, namely smooth rebar, widely and often unequally spaced ties (200 to 250 mm), and 90° hooks. The wide spacing of the ties resulted in shear failures (Figure 3-26), buckling of longitudinal rebar (Figure 3-27), and poor confinement of the core concrete (Figure 3-28).



Figure 3-27 Shear failure of a moment-frame blade column



Figure 3-28 Lack of transverse reinforcement in moment-frame column

Shear failures in short columns were common. A typical example of such a failure is a school building in Adapazari, shown in Figure 3-29. The damaged column of Figure 3-29b is shown in Figure 3-29a in a blue circle.



Figure 3-29 Shear cracking in short columns

a. building elevation

b. diagonal cracking in column

Column-infill masonry wall interaction resulted in severe damage to and failure of many moment-frame columns. Consider the building east of Gölcük that is shown in part in Figure 3-30. The infill hollow clay tile masonry on each side of the central column in this figure failed completely and the column hinged at each end. The column to the left of the central column was captured approximately 1 m above the floor by the residual hollow clay tile. The shear cracks that were observed in this captive column formed in the column at the top face of the remaining infill masonry.



Concentrated damage at the ends of moment-frame columns was observed throughout the epicentral region. Examples of such damage are presented in Figures 3-31, 3-32, and 3-33. Large rotations at the ends of the columns (Figure 3-31) produced severe cracking and loss of concrete. (Note the relative proportions of the columns and the beam in this figure.) Out-of-plane deformations in the column of Figure 3-32a led to loss of cover concrete in the hinging zone. The transverse ties in this column were widely spaced (200 mm) and composed of

smooth rebar with 90° hooks. Such connection details have limited rotation capacity. The beam and slab framing (Figure 3-32b) lost seating on

the column. The first-story columns of a collapsed building are shown in Figure 3-33; the second-story of the building is to the left of the columns. Note the smooth failure surface on the top right side of the columns.



Figure 3-31 Concentrated damage at ends of moment-frame columns due to excessive drift



a. damage from out-of-plane deformation



b. unseating of beam-slab system from column

Figure 3-32 Damage and failures at ends of moment-frame columns

3.5.3 Beam-Column Joints

Typical damage to beam-column joints is shown in Figures 3-34, 3-35, and 3-36. The collapse of a building in Adapazari (Figure 3-35) was due to the failure of beam-column joints. Much of the framing (Figure 3-35a) is essentially intact but many of the beam-column joints are heavily damaged. One of the damaged joints is shown in Figure 3-35b. Beam rebar anchorage in the joint is inadequate and no transverse ties are present in the joint.

Figure 3-36 is a photograph taken in a building under construction in Adapazari at the time of the earthquake. Severe damage in the beam-column joints is evident, but horizontal transverse ties in the joints maintained the integrity of the joints. (See Section 3.7.3 for a more complete description of this building.)



Figure 3-33 Damage to moment-frame columns



Figure 3-34 a. Damage to moment-frame beam-column joints

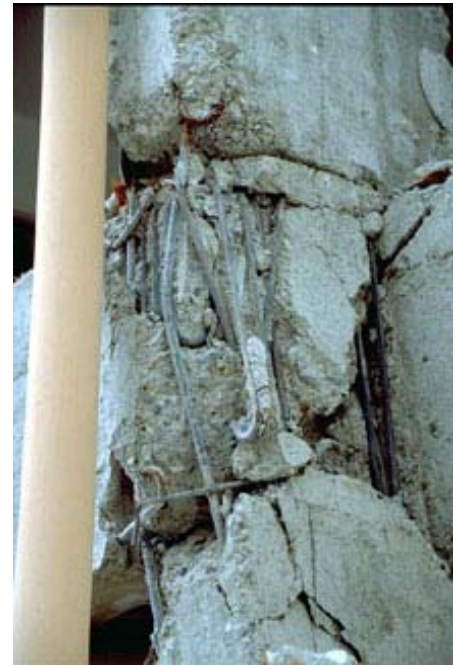


Figure 3-34 b. Damage to moment-frame beam-column joints, reinforcement in joint



Figure 3-35 a. Building collapse due to failure of beam-column joints



Figure 3-35 b. Damage to one beam column joint

Figure 3-36 is a photograph taken in a building under construction in Adapazari at the time of the earthquake. Severe damage in the beam-column joints is evident, but horizontal transverse ties in the joints maintained the integrity of the joints. (See Section 3.7.3 for a more complete description of this building.)



Figure 3-36 Damage to a new moment-frame beam-column joint

3.5.4 Asmolen Slab Floor System

The asmolen slab floor system, described in Section 3.3.2, is commonly used in the epicentral region. In this type of construction, the hollow clay tile, which is used as permanent formwork, is not positively attached to the slab or the joist-beam framing.



Figure 3-37 Typical damage to asmolen floor systems

Damage to such systems was widespread. Figure 3-37 shows typical damage to the asmolen floor system. Deformation of the joist-beam framing led to sections of the hollow clay tile formwork dislodging and falling to the floor below. Although failure of the hollow clay tile blocks in the floor system is not considered structural damage, falling tile blocks constitute a hazard to life.

3.6 Shear-Wall Construction

Buildings constructed using shear walls as the primary lateral load-resisting system performed quite well in the 1999 Izmit earthquake. Some buildings with a dual wall-frame lateral load resisting system were damaged because the shear walls were not sufficiently stiff to keep the deformations of the nonductile framing system in the elastic range. Story collapses were not observed in buildings containing a substantial number of shear walls, but it should be noted that shear walls were not widely used in the epicentral region.

3.6.1 Behavior of Shear-Wall Construction

Outside Istanbul, few buildings in western Turkey are constructed with shear walls as the primary lateral load-resisting system. However, those wall buildings in the epicentral region, such as the building under construction in Figure 3-38 and the apartment buildings of Figure 3-39, performed well. Shear walls were used as the lateral load-resisting system in both the transverse and longitudinal directions of the building in Figure 3-38. This building suffered minor damage to the infill walls. The lateral force-resisting systems in the two apartment buildings shown in Figure 3-39 included moment-frames along the major axis of the buildings and shear walls along the minor axis. These buildings

were located in a residential area near Gölcük where all of the nearby moment-frame apartment buildings collapsed (see Figure 3-12).



Figure 3-38 Shear wall building under construction at the time of the earthquake



Figure 3-39 Undamaged apartment building in Gölcük

The building shown in Figure 3-40 experienced damage at the stiffness discontinuity in the shear wall. The fault ruptured directly beneath this building. The limited damage in this instance constitutes excellent performance.



Figure 3-40 a. Shear wall building damaged due to fault rupture



Figure 3-40 b. Close up of damage to a shear wall

The reconnaissance team toured a number of buildings that would be classed as dual wall-frame systems in the United States. However, because design provisions for such systems did not exist in Turkey prior to 1997, these buildings would have been designed as either shear walls or moment-resisting frames. The most significant damage observed by the team in a dual wall-frame building is shown in Figure 3-41a. The wall and first-story exterior columns shown (Figure 3-41b) failed and shortened. These components displaced out of the plane of the wall, as seen in Figure 3-41b.



Figure 3-41 a. Collapse of dual wall-frame five story building, Adapazari



Figure 3-41 b. Close-up of failure of the shear wall and perimeter columns



Figure 3-42 a. Damaged wall-frame building due to ground failure and wall rotation



Figure 3-42 b. shear wall settlement

Another example of damage to beams and columns in a dual wall-frame building is shown in Figure 3-42. No cracks were observed in the shear wall, but the right end of the wall settled approximately 0.5 m (Figure 3-42b) due to bearing failure of the supporting soils. Although the shear wall was likely sufficiently stiff to protect the nonductile frame, the rotation at the base of the shear wall and settlement of the footings beneath the moment-frame columns contributed to the failure of the first-story columns.



Blade columns or short shear walls were often constructed near stairwells (Figure 3-43). These walls or blade columns were detailed similarly to regular moment-frame columns with light transverse reinforcement with 90° hooks and no cross ties. The failures shown are similar to those observed in moment-frame columns.

Figure 3-43 Damage to short wall / blade column

3.7 Performance of Selected Buildings

Modern standards for the seismic evaluation of buildings (FEMA 1997) dictate decisions regarding system response using information on component response. For the system performance level of collapse prevention, system failure is linked to the first failure of a component (typically measured in terms of deformation demands or demand-capacity ratios). Such correlation of system and component response is misleading and often overly conservative if the seismic and gravity load-resisting systems are redundant. One objective of the reconnaissance team was to gather information related to limiting states of response of building systems, with an emphasis on the limit state of collapse prevention. The following sections describe in some detail the performance of four buildings: A through D. The first three buildings (A, B, and C) sustained severe damage to critical components but did not collapse. The fourth building (D) performed poorly but as a result of ground failure.

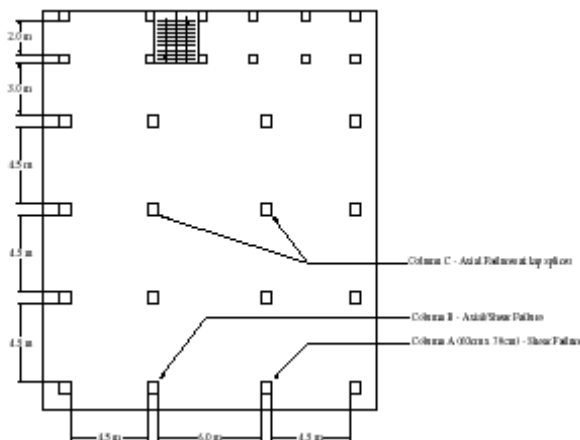
3.7.1 Building A



Figure 3-44 Front elevation of Building A



Figure 3-45 Rear elevation of Building A showing intact infill masonry walls



3.7.1.1 Description

Building A, shown in Figures 3-44 and 3-45, was located at the eastern outskirts of Gölcük. Much of the first story of this moment-frame building (not seen in Figure 3-44) was located below grade. The grade level sloped down from the front to the back of the building. A sketch of the first-floor plan of the building is shown in Figure 3-46. Most of the hollow clay tile infill masonry failed during the earthquake but some remained intact at the rear of the building in the sixth story (see Figure 3-45).

3.7.1.2 Component Failures

Structural damage was concentrated in the first-story columns at the front of the building (Figure 3-47) and around the stairwell at the rear of the building (Figure 3-48). Nonductile detailing was evident in each damaged component viewed by the reconnaissance team.



Figure 3-47 Damage to first story columns



Figure 3-48 Damage at the rear stairwell

The staircases in the rear stairwell were cast integrally with the exterior columns. The landings were located approximately 1 m below the beam-column joints (Figure 3-48). No transverse reinforcement was present in these joints. The lateral support provided by the landings and the staircases resulted in short column construction and led to shear failures immediately above the landings. Figure 3-48 shows severe damage to the staircases that suggests that the staircases resisted significant lateral forces during the earthquake via strut action. The lateral stiffness of the staircases is

evinced by the damage they suffered but likely was not included in the earthquake analysis of the building (which is also common practice in the United States).

The distribution of damage to columns in the first story is shown in Figure 3-46. Figures 3-49, 3-50, and 3-51 show column failures. Nonductile detailing is evident, including widely spaced perimeter transverse ties with 90° hooks and no cross ties, and lap splices located at the floor level with no confining transverse reinforcement.



Figure 3-49 Shear failure of Column A (See Figure 3-46)



Figure 3-50 Axial failure of column B (See Figure 3-46)



Figure 3-51 Axial failure at lap splice in Column C (See Figure 3-46)

3.7.1.3 System Response

A comprehensive performance-based evaluation methodology should be able to predict distributions of damage similar to that identified above assuming an accurate characterization of earthquake shaking. The performance of Building A brings into question the procedures currently adopted in the United States for system evaluation for the performance level of collapse prevention. (In this report, “collapse” is defined in terms of the failure of the gravity load-resisting system.)

As shown in Figures 3-46 and 3-47, the first and third rows of columns were badly damaged but the second row of columns suffered no significant damage. All columns in the first three rows were the same size; rebar in the first and third rows of columns were essentially identical. If the interior columns in the first row failed initially, conventional approaches would suggest that lateral forces were redistributed to other stiff components (including the second row of columns) and gravity loads were transferred to the undamaged columns in the first and second rows. The increase in the gravity and earthquake effects should have been greater on the second-row columns than on the third-row columns, yet the columns in the third row failed and the columns in the second row were undamaged. New knowledge regarding the transfer of lateral loads and gravity from failed components to other components of a building frame is needed to obtain accurate estimates of building performance.

Although several columns in the first story of the building failed in shear and axial compression, the building did not collapse. Clearly system response cannot be judged on the basis of the most highly loaded (forces or deformations) component in the building, as is the practice in FEMA 273, *NEHRP Guidelines for the Seismic Rehabilitation of Buildings* (FEMA 1997). The gravity load-resisting system of the building did not collapse for a number of reasons that include (a) frame action in the stories above the damaged columns and (b) residual axial-load capacity in the heavily damaged columns.

After the columns in the first row failed in shear and shortened, the slab and beam framing deflected in the shape of a catenary (see the sag in the floor slabs in Figure 3-44) and gravity loads were carried to the adjacent undamaged columns by axial tension in the beams and slabs. Vierendeel truss action in the upper stories also likely transferred gravity loads to adjacent undamaged columns. Provision for such redundancy in framing systems would reduce the likelihood of building collapse and substantially uncouple system-level response from component-level response. The catenary and Vierendeel truss mechanisms may be very effective in stabilizing the structure when interior columns are lost. To ensure that beams and slabs are able to maintain catenary deflections, bottom reinforcement should be continuous through any columns that may fail under lateral loads.

Recent studies (Moehle et al. 2000) have shown that columns heavily damaged in shear are still capable of supporting axial loads. Residual axial strength in these columns would reduce the need to redistribute gravity loads as described in the previous paragraph. The failed columns in the first row were squat so that after failure in shear, the upper segments of the columns bore on the lower segments, albeit not concentrically. (Contrast this behavior with that described earlier for narrow columns; see Figure 3-32). The core concrete in the failed columns in the third row continued to carry gravity loads after the earthquake because the cores of the columns remained partially intact. The use of transverse reinforcement in the amount needed to keep the core of a column intact at large deformation would further reduce the likelihood of building collapse.

3.7.2 Building B



3.7.2.1 Building Description

Building B (Figure 3-52) was located 5 km east of Gölcük. The six-story reinforced concrete frame building was unoccupied at the time of the earthquake. The footprint of the building was approximately 12 m by 16 m.

Figure 3-52 Elevation of Building B

3.7.2.2 Component Failures

A corner column in the third story of Building B failed during the earthquake, as seen in Figure 3-52. Part of the roof framing of the adjacent building can be seen immediately below the failed column, indicating that the third-story column failed due to the impact of the adjacent building. Figure 3-53 shows more details of the failed column and the roof slab of the adjacent building.



Figure 3-53 Details of damage to third-story column of Building B

3.7.2.3 System Response

Although one column in the third story of the building was completely destroyed due to impact of the roof slab of the adjacent building, the building did not collapse. The gravity load-resisting system in the building did not collapse because of frame action in the stories above the destroyed column. The performance of Building B also raises a number of questions once again about the procedures currently adopted in the United States for system evaluation for the performance level of collapse prevention. The performance of Building B raises the questions: (1) should component loss be accounted for in the design of the building for the performance level of collapse prevention? and (2) If so, how?

The loss of one or more components in a moment-frame building can substantially modify the magnitude and behavior of the remaining components. Assuming that the location(s) of the failed component(s) are known, nonlinear methods of analysis can be used to evaluate the forces and deformations in the damaged building frame. Two challenges with such analysis are (1) identifying the number and locations of components to be removed from the mathematical model and (2) including the effects of column failure and load redistribution.

Procedures for selecting the number and locations of components to be removed from the mathematical model have not been developed. The number and locations will vary as a function of the earthquake histories used for analysis and evaluation. Demand-to-capacity ratios (deformations for ductile actions and forces for nonductile actions) could perhaps be used to identify combinations of components for removal from the mathematical model. Two approaches could be used to assess

system response following the failure of selected components: (1) remove the components from the mathematical model before analysis and (2) remove the components from the model during the analysis when deformations or forces, or demand-capacity ratios exceed a threshold value. Approach 1 is more conservative than Approach 2. Approach 1 could be used with nonlinear static or dynamic analysis. Approach 2 would be used only with nonlinear dynamic analysis.

The rapid loss of a column or beam can lead to a dynamic amplification of the gravity loads that are transferred to adjacent components. Procedures for calculating the amplification factor are not available at this time. Studies are very recently completed at PEER by Rodgers and Mahin on steel moment-frame buildings and by Elwood and Moehle on nonductile reinforced concrete moment-frame buildings to evaluate the effect of component failure on system response.

3.7.3 Building C



3.7.3.1 Building Description

Building C, shown in Figure 3-54, was located near the Adapazari city center. The five-story reinforced concrete frame building included a high retail space in the first story. The retail space shown in Figure 3-55 included a mezzanine level on the west side of the building. The building was not occupied at the time of the earthquake.

Figure 3-54 Elevation of Building C

3.7.3.2 Component Failures

Most of the first-story columns connected to the mezzanine level failed in shear (Figure 3-55). The mezzanine level reduced the clear length of the columns, resulting in shear failures before the moment capacities of the columns could be developed. Damage to the stair framing and short shear wall connected to the mezzanine level can also be seen.

One of the failed columns at the rear of the building had a very steep shear crack (Figure 3-56) that suggested that the column was carrying high axial loads. Following a more detailed inspection of the building, the reconnaissance team concluded that the column was part of a two-story addition, which was separated from the five-story building by an expansion joint. No plausible explanation for the steep shear crack is proposed. The beam-column joints at the top of the first-story columns on the eastern façade were damaged but did not fail because transverse reinforcement was provided in the joint region; see Figure 3-57. The beam-column joint at the north-east corner of the first story was heavily damaged, as shown in Figure 3-58, but continued to carry gravity loads.



Figure 3-55 View of retail space in the first story of the Building C



Figure 3-56 Shear crack in the first story column in the rear of Building C



Figure 3-57 Damaged beam-column joints at top of first story columns, Building C



Figure 3-58 Damaged beam-column joint at top of first-story corner column, Building C.

3.7.3.3 System Response

The residual drift in the first story of the building was approximately 300 mm to the east. Although the building to the west of Building C overturned due to bearing failure of the soils beneath its 1-m-thick foundation, soil deformation and failure did not appear to contribute to the damage in Building C.

To predict incipient collapse of a building or to evaluate buildings for the performance level of collapse prevention, new information on how gravity loads are supported in buildings with severely

damaged or failed components is needed. The severely damaged interior columns of Figure 3-55 could support little or no gravity load. This observation suggests that much of the gravity load in the building must have been distributed to the perimeter first-story columns by Vierendeel truss action in the upper stories. Many of these perimeter columns suffered damage to their beam-column joints, but the use of transverse reinforcement prevented joint failure and gravity load resistance was maintained.

Although the residual drift of the first story of the building adjacent to the front sidewalk was approximately 5%, the $P - \Delta$ effects did not lead to collapse of the building. Three factors probably contributed to the stability of the building. First, the shear wall near the stairwell (see Figure 3-55), although heavily damaged, likely had significant residual lateral stiffness and strength. Second, the axial loads in the columns were low as a percentage of $f_c'A_g$. Third, the residual drift at the rear of the five-story building was much less than 5% and the framing at the rear of the building may have partially stabilized the building.

3.7.4 Building D

3.7.4.1 Building Description

Building D was a six-story moment-frame building located in the center of Adapazari. An elevation of the building is shown in Figure 3-59. Based on similar construction of the same age in Adapazari, the foundation for Building D was probably a mat or raft with a thickness of approximately 1 m.



Figure 3-59 Elevation of Building D

3.7.4.2 System Response

Building D is an example of poor system performance that was not accompanied by component damage or failure. This building suffered little damage as a result of the earthquake shaking but could not be occupied because it settled more than 1 m due to liquefaction and bearing failure of the supporting soils (see Figure 3-60). It is likely that this failure of the supporting soils limited the shaking experienced by the building. Services and utilities to the building were destroyed and ingress and egress were most difficult. The poor performance of this building underscores the need to

explicitly account for soil and foundation behavior in performance-based earthquake engineering. Although the building would have satisfied the performance level of collapse prevention (as defined in FEMA 273 [FEMA 1997] and Vision 2000 [SEAOC 1995]), it would not have satisfied the egress requirements of the life-safety performance level. To achieve performance beyond collapse prevention, site improvements to avoid liquefaction would have been required.



Figure 3-60 Settlement of Building D due to liquefaction and soil-bearing failure

3.7.5 Summary Remarks

The purpose of the discussion of selected buildings is to identify issues relating to building performance that must be addressed in the development of guidelines and tools for the implementation of performance-based earthquake engineering.

At the time of this writing, building (system) response is often judged on the basis of the most highly damaged component in the building. Clearly, this approach, although conservative, is neither accurate nor cost effective. Poor behavior of one or two random components does not necessarily lead to poor system behavior, although poor behavior of one or two key components may lead to system collapse if mechanisms for redistribution of gravity loads do not exist in a building.

Much remains to be learned about the collapse of buildings and the design of buildings on soils prone to liquefaction or failure. Research on the following topics is needed to improve analysis,

evaluation, and design procedures to ensure with high confidence and low cost that buildings will not collapse.

1. Triggers for axial load failure of ductile and nonductile reinforced concrete columns under combined loadings based on large- or full-scale test data.
2. Mechanisms for redistribution of gravity loads in the event of component(s) failure, and characterization of gravity-load amplification effects due to component failure.
3. Analytical tools for predicting component strength and stiffness loss under combined loadings based on evaluation of large-scale experimental data.
4. Procedures for eliminating components from mathematical models to simulate component failures.
5. Large-scale 3-D earthquake simulator testing of buildings with weak and brittle components to validate the analysis, evaluation, and design procedures developed in 1 through 4 above.

*Editors note: This text follows as closely as possible from the paper copy of Chapter 3 “Reinforced Concrete Frames and Wall Buildings” by H.Sezen et al. **Structural Engineering Reconnaissance of the Kocaeli (Izmit) Turkey Earthquake of August 17 1999**. Berkeley: Pacific Earthquake Engineering Research Center, (PEER Report 2000-09), December 2000. A few figures have been substituted where color originals did not exist. Minor text and layout modifications were made. Higher resolution images of all images are available through EQIIS image database <http://nisee.berkeley.edu/eqiis.html> by searching under the “[Izmit \(Kocaeli\), Turkey earthquake, Aug. 17, 1999](#)”*
C. James, 2001

4 Industrial Facilities

4.1 Overview of Construction and Damage

4.1.1 Introduction

Several areas of concentrated heavy industry surround the Sea of Marmara and Izmit Bay, extending west to Adapazari; approximately 40% of heavy industry in Turkey was located here before the earthquake. Figure 4-1 is a map of the eastern end of Izmit Bay showing the locations of several cities mentioned in the remaining sections of this chapter. Figure 4-2 is an aerial photograph of Körfez looking west along Izmit Bay. Extensive damage to many industrial facilities was observed over a wide strip that was centered on the fault line.

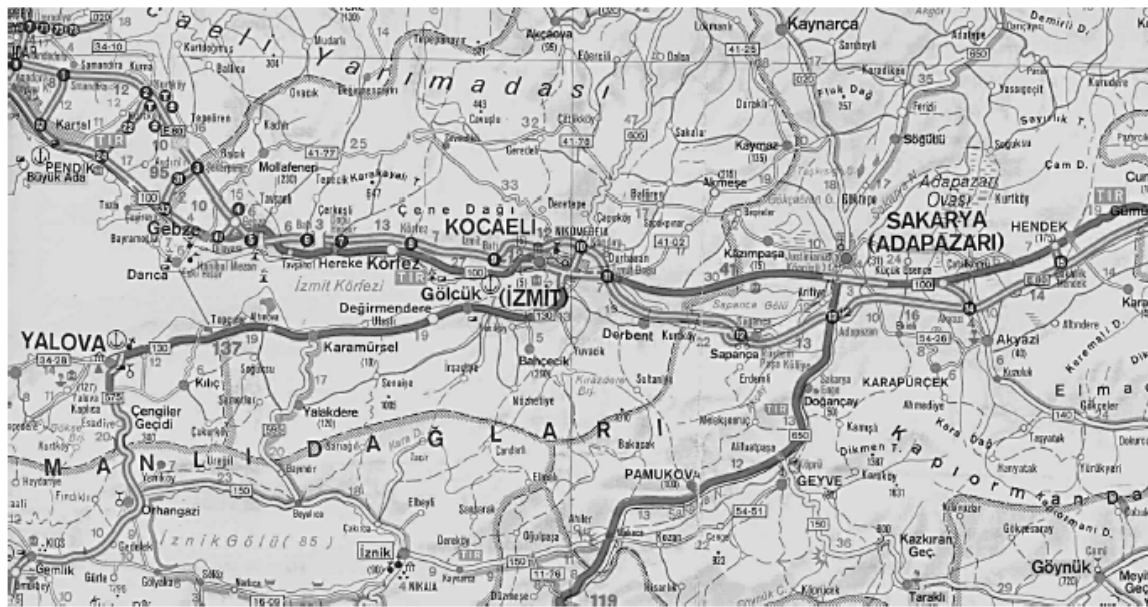


Figure 4-1 Map of the eastern end of Izmit Bay

Twenty-four facilities representing different industries in the İzmit and Adapazari regions were surveyed in the weeks following the earthquake. Since many of these facilities were designed according to current U.S. and European standards, their performance is relevant to other seismically active regions of the world. The following sections summarize observations from some of those industrial facilities visited by members of the PEER reconnaissance team. An alphabetical list of the facilities visited by the reconnaissance team, relevant construction information, and an approximate number of employees are presented in Table 4-1. The construction date for facilities under construction at the time of the earthquake is listed as 1999+ in the table; zero employees are listed for these facilities.

The managers of the industrial facilities visited by the reconnaissance team were most generous in granting the team permission to tour damaged buildings and structures. In a number of facilities permission to enter was granted on the clear understanding that no photographs be taken. A number of these facilities are described in the following sections but no photographs are presented.



Figure 4-2 Aerial photograph of industrial facilities in Körfez looking west

The widespread damage to industrial facilities had a substantial impact on the economy of the region, measured here in terms of direct and indirect losses. Direct losses were a result of structural damage and nonstructural damage, including damage to mechanical, electrical, and plumbing systems. For the purpose of this report, classification schemes for structural and nonstructural damage were developed; these schemes are presented in Tables 4-2 and 4-3, respectively. The observed structural and nonstructural damage to the facilities of Table 4-1 are listed in Table 4-4.

The following three subsections present summary information on typical industrial-facility construction practice in Turkey, followed by information on damage to petrochemical facilities, automotive facilities, power generation and transmission facilities, and assorted industrial facilities.

Table 4-1 Industrial facilities visited by the PEER reconnaissance team

<i>Facility</i>	<i>Function/Product</i>	<i>Construction Date</i>	<i>Construction Type¹</i>	<i>Employees</i>
Adapazari Substation	Power distribution	—	Assorted	NA
Bastas	Fluorescent tubes	1960s	RC	NA
BekSA	Steel cord	1987	RC	240
BriSA	Tires	1974, 1989	RC	100
Çamlica	Soft Drinks	1999+	RC	NA
Çap Textile	Textiles	1997	RC	650
Çiti	Glass vials	NA	RC	NA
DuSA	Chemicals	1987	Assorted	NA
DuSA	Chemicals	1999+	Steel	NA
EnerjiSA	Power	1997	Steel	50
Ford	Automotive	1999+	RC	NA
Goodyear	Tires	1963	Steel	500
Habas	Liquid gases	1995	Assorted	NA
Hyundai	Automobiles	1997	Steel	850
KordSA	Tire cord	1973	Steel	1100
Mannesmann	Pipe	1955	Steel	200
Pakmaya	Food processing	1976	Steel	300
Petkim	Petrochemical	1967-1975	RC	2500
Pirelli	Tires	1962	RC	900
SEKA	Paper Mill	1936-1960	RC	NA
Toprak Drug	Drugs	1990	RC	240
Toprak Clean	Cleaning supplies	1993	RC	250
Toyota	Automobiles	1994	Steel	NA
Tüpras	Refinery	1961	Assorted	1350

1. Assorted = steel and reinforced concrete; RC = reinforced concrete
 NA = not available

Table 4-2 Structural damage classification

<i>Level</i>	<i>Damage</i>	<i>Function</i>	<i>Repair</i>	<i>Typical Damage</i>
1	None	Fully operational	None	Negligible
2	Minor	Partially operational	Minor	Minor cracks in RC components; bolt failures in steel frames.
3	Moderate	Out of operation for days or several weeks	Modest repair	Significant cracks in RC components; yielding in steel moment frames
4	Major	Out of operation for months	Major repair or replacement	Spalling and crushing of RC components; fracture of rebar in RC components; anchorage failure in precast RC components; buckling of braces in steel frames; fracture of steel moment frames; modest permanent drift of building frame
5	Collapse	None	Not possible	Multiple component failures; part or full loss of floors or roofs; gross distortion of steel frames; large permanent drifts

Table 4-3 Nonstructural damaged classification

<i>Level</i>	<i>Damage</i>	<i>Function</i>	<i>Repair</i>	<i>Typical Damage</i>
1	None	Fully operational	None	Negligible
2	Minor	Partially operational	Clean up	Small movement of unanchored equipment; overturning of cabinets and shelved products
3	Moderate	Out of operation for days or several weeks	Engineered repair	Modest damage to architectural, mechanical, electrical, and plumbing systems; failure of equipment anchorage and movement of equipment.
4	Major	Out of operation for months	Major repair or replacement	

Table 4-4 Damage to industrial facilities visited by the PEER reconnaissance team

<i>Facility</i>	<i>Construction Date</i>	<i>Construction Type¹</i>	<i>Structural Damage¹</i>	<i>Nonstructural Damage²</i>
Adapazari Substation	—	Assorted	1	4
Bastas	1960s	RC	1	4
BekSA	1987	RC	4	3
BriSA	1974, 1989	RC	4	3
Çamlica	1999+	RC	4	3
ÇapTextile	1997	RC	5	4
Çiti	NA	RC	3	3
DuSA	1987	Assorted	4	4
DuSA	1999+	Steel	1	NA
EnerjiSA	1997	Steel	2	3
Ford	1999+	RC	3	NA
Goodyear	1963	Steel	2	3
Habas ³	1995	Assorted	5	4
Hyundai	1997	Steel	4	4
KordSA	1973	Steel	3	3
Mannesmann	1955	Steel	3	3
Pakmaya	1976	Steel	4	4
Petkim	1967-1975	RC	5	3
Pirelli	1962	RC	4	3
SEKA	1936-1960	RC	4	4
Toprak Drug	1990	RC	2	4
Toprak Clean	1993	RC	3	4
Toyota	1994	Steel	1	2
Tüpras	1961	Assorted	5	4

1. See Table 4-2 for information on structural damage.

2. See Table 4-3 for information on nonstructural damage.

3. Two of three tanks completely destroyed; unknown nonstructural damage inside the undamaged tanks.

4.1.2 In-Situ Reinforced-Concrete Structures

In-situ reinforced concrete beam-column frame construction is common in smaller and older industrial facilities in Turkey. The quality of the construction in these facilities was typically substantially better than the quality of residential or commercial construction. Of the 24 facilities visited by members of the PEER reconnaissance team, 14 were constructed with reinforced concrete moment-resisting frames. Most of the damaged in-situ concrete structures viewed by the reconnaissance team were constructed without the use of modern ductile details.

4.1.3 Prefabricated Reinforced-Concrete Structures

For reasons of economy and speed of construction, prefabricated or precast reinforced concrete members are used commonly for the construction of industrial facilities. Typical spans in the facilities visited by the reconnaissance team varied between 15 m and 25 m. The typical height of these precast structures ranged between 6 m and 8 m.

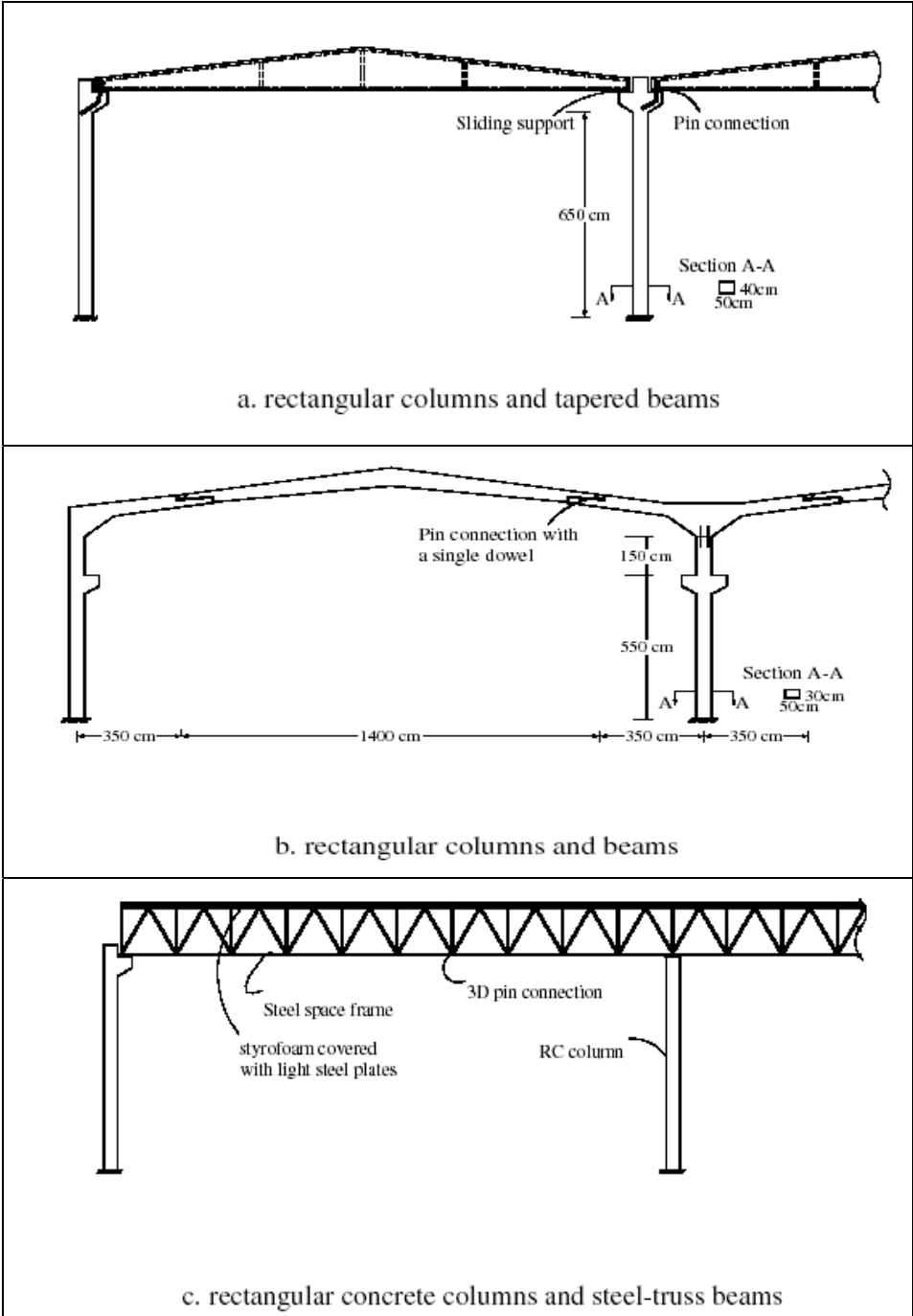


Figure 4-3 Prefabricated reinforced concrete construction

Three of the popular precast structural systems in Turkey are shown in Figure 4-3. The frame of Figure 4-3a is composed of individual columns and long-span rectangular or tapered beams, each

with a pinned support at one end and a sliding support at the other end. The typical spacing of these frames was approximately 6 m. The pinned support was typically composed of one or two anchorage dowels, which served to prevent lateral movement but permitted rotation. The sliding support permitted lateral displacement and rotation. Typical plan dimensions of columns in these frames were 400 mm x 400 mm to 500 mm x 500 mm. Reinforced concrete planks spanned between the frames and were supported on pockets cast into the precast beams. Typical plank construction and a damaged dowel connection are shown in Figure 4-4; the beam and slab on the right-hand side of the column were close to collapse. Substantial damage and a lack of transverse reinforcement are evident in the column and beam corbels. Fixity at the base of the columns of Figure 4-3a was achieved by grouting the column in a deep socket or footing that was linked to other footings by grade beams and a thick slab at the top of the foundation. Typical interior and exterior foundation socket-column base details are shown in Figures 4-5a and 4-5b, respectively. The grade beams between the exterior socket foundations can be seen in Figure 4-5b. (The 6.5-m high columns in the Çamlıca Soft Drink production facility [Figure 4-3a] were reported to be installed in 4-m-deep socket foundations.)



Figure 4-4 Typical plank roof construction and damaged doveled connections

Another common prefabricated structural system in this part of Turkey is shown in Figure 4-3b. This system includes a precast T-shaped member at the top of the central column that serves to connect the column to simply supported roof beams. The connection of the T-shaped unit to the column is detailed to transfer moment and shear, but likely for gravity-load effects only. The lengths of the T-shaped unit and the simply supported roof beams are selected on the basis of gravity-load actions in a two-span continuous beam; namely, the doveled connections between the units are located at the points of contraflexure. Such an approach would minimize the volume of material in the roof beams for gravity-load effects only. Figure 4-6 shows damage to a steel pipe production facility, which was under construction at the time of the earthquake. The roof panels had not been installed, and as such there was no diaphragm at the roof level. The seismic load paths in this building, both parallel and perpendicular to the frames of Figure 4-3b, would have been questionable even if the roof panels had been installed. As is evident in the figure,

many of the columns acted as cantilevers and hinged at their bases during the earthquake. The precast T-units of Figure 4-3b rotated off the top of the two central columns in the middle of the photograph Figure 4-6 and are upside down. There was minimal reinforcement joining the T-shaped units to the columns below.



a. interior foundation socket connection



b. exterior foundation socket connection

Figure 4-5 Foundation connection for prefabricated reinforced concrete facilities

A cross section through a third prefabricated framing system in use in Turkey at the time of the earthquake is shown in Figure 4-3c. The gravity-load framing system in this figure is composed of a light steel (3-D) space frame that is supported by steel trusses that span between the precast reinforced concrete columns. Socket foundations of the type shown in Figures 4-5a and 4-5b were typically used for the precast columns. Such construction was somewhat common in modern facilities constructed by joint ventures of Turkish and international companies, such as the KordSA, BekSA, Ford, and Toprak Cleaning facilities.



a. failed central columns and T-shaped units

Figure 4-6 Damaged precast reinforced concrete framed building

4.1.4 Steel-Frame Structures

Braced and moment-resisting steel frames are used for some single-story and many multistory industrial facilities. One such facility, under construction at the time of the earthquake for DuSA, is shown in Figure 4-7. The framing system in this five-story building suffered no damage but much of the reactive weight in the form of the concrete-on-metal deck floors and masonry perimeter walls was not present at the time of the earthquake. The building was designed and detailed in the United States using U.S. standards for such facilities. The seismic moment-resisting frame in the elevation of (Figure 4-7a) used bolted end-plate connections. On the perpendicular elevation (Figure 4-7b), eccentrically braced steel frames were used to resist seismic loads. On this elevation, part of a three-story masonry wall peeled off the exterior steel framing and collapsed; the remaining part of the wall can be seen to the right of the crane base.



a. elevation showing steel moment frames



b. elevation showing steel eccentrically braced frames

Figure 4-7 Five-story steel-framed industrial facility under construction

4.2 Petrochemical Industry

4.2.1 Introduction

There is a heavy concentration of petrochemical facilities near Körfez on the northern side of Izmit Bay. Many of the badly damaged facilities were located within 15 km of the epicenter where levels of earthquake shaking were moderate to high. The fiscal health of many of the companies operating these facilities is highly dependent on an adequate supply of raw materials, and product from other industrial facilities in the region. The failure of or gross damage to some facilities in the epicentral region had a cascading fiscal effect on other businesses in the region. The Tüpras refinery (Section 4.2.2) and the Petkim petrochemical plant (Section 4.2.3) were two such facilities.

4.2.2 Tüpras Refinery

4.2.2.1 Introduction

The most spectacular damage to an industrial facility was observed at the state owned and managed Tüpras oil refinery near Körfez (see Figure 4-8: a photograph taken shortly after the earthquake by an unknown photographer). Prior to the earthquake, the Tüpras refinery produced more than 200,000 barrels of oil-related product per day, approximately one-third of Turkey's total output. The Tüpras product was primarily for domestic consumption, much of which was local to industry in the Körfez region. The Tüpras refinery was designed and constructed in the early 1960s by U.S. contracts and according to U.S. standards of practice at that time (Danis 1999). As such, the damage observed to the Tüpras refinery would not be unexpected at refineries of a similar age that are located on the West Coast of the U.S. The plant was expanded in size and production in 1974 and 1983.



Figure 4-8. Tank farm fires at Tüpras refinery



Figure 4-9. Tüpras refinery showing part of the tank farm



Figure 4-10. Tupras refinery



Figure 4-11. Loading and unloading jetty at Tupras refinery

The damage to the Tüpras refinery was widespread and included port facilities, storage tanks, cooling towers, stacks, and crude-oil processing units. Much of the damage was fire related: an indirect consequence of the earthquake shaking. The fire-fighting capability of the refinery was lost immediately following the earthquake because of multiple ruptures of the water pipeline from Lake Sapanca, 45 km east of the refinery. (The refinery received all of its water from this lake.) In the days immediately following the earthquake, the resulting fires were contained by aerial bombardment with foam (Danis 1999). At the height of the conflagration, a 3-km region around the refinery was evacuated (Danis 1999). The fires were extinguished by water drawn from Izmit Bay by using portable diesel pumps and flexible hose that didn't arrive at the refinery until three days after the earthquake. Had this fire-fighting equipment been stockpiled at the refinery in advance of the earthquake, the fires that took five days to extinguish would have been put out much sooner. For information, the reconnaissance team visited the Tüpras refinery on September 1, 1999, two weeks after the earthquake and approximately ten days after the fires had been extinguished. (Valuable lessons for refineries on the West Coast of the U.S. can be learned from the problems encountered by the fire-fighting and emergency-response staff at the Tüpras refinery.)

Figures 4-9, 4-10, and 4-11 are aerial photographs of the refinery taken by members of the reconnaissance team two weeks after the earthquake. Figure 4-9 shows the main processing facility and part of the tank farm (in the foreground). The jetty that serviced the refinery is not shown but is located at the left-hand edge of the figure. Another view of the main processing facility shows the failed heater stack (see the circled section in Figure 4-10). Some of the burned fuel-oil tanks can be seen in the upper right middle of the figure. The remains of the timber cooling tower that burned following the earthquake can be seen in the middle right of the photograph between the burned tanks and the northern perimeter of the main processing facility. Substantial pollution can be seen (Figures 4-9 and 4-10), which resulted from the failure and breaching of fuel-oil tanks, much of which was successfully contained by the earthen berms that surrounded the tanks. According to refinery staff, some oil spilled into Izmit Bay due to fractured pipes and from an oil tanker that pulled away from the loading jetty immediately following the earthquake.

4.2.2.2 Loading Jetty

The loading and unloading jetty shown in the aerial photograph (Figure 4-11) serviced the refinery only. Failure of this jetty prevented the loading and unloading of all fuel-oil products at the refinery. Ships tied up to the long arm of the T-shaped jetty (oriented north-west to south-east in the figure, where the top of the page is north). The jetty was composed of a reinforced concrete deck that was supported on steel piles. Modest ground failure was observed around the approach to the jetty. The support to the crude-oil pipeline (Figure 4-12) that ran along the seawall near the jetty was lost. Figure 4-13 is a photograph of the damaged jetty from point A of Figure 4-11. Gross damage to the jetty and the elevated pipeway and pipes is evident to the left of the tug. These pipes transferred fuel oil and other products between the refinery and ships tied to the jetty. Figure 4-14 is a photograph of the damaged jetty, from point B of Figure 4-11, that resulted from the failure of some of these piles. The loading and unloading jetty was separated from the vertical leg of the jetty. Refinery staff told members of the reconnaissance team that the heavy steel grating joining the two components of the jetty dropped into the water, indicating that the two components moved independently during the earthquake. The reconnaissance team observed steady leaks from one of the pipes at ground level, which was filled with volatile gasoline, more than ten days after the earthquake.



Figure 4-12. Failed crude oil pipeline along the sea wall at the Tupras refinery



Figure 4-13. Damaged loading and unloading jetty



Figure 4-14. Damage to jetty and elevated pipeway in Tupras refinery

4.2.2.3 Tank Farms and Floating Roof Tanks

Because fires burned out of control for several days in the tank farms, international attention was focused on the Tüpras refinery immediately following the earthquake. Refinery staff reported that the first major fire ignited in a floating-roof tank that contained naphtha, which is a highly volatile flammable liquid mixture distilled from petroleum. The fire reportedly spread quickly because the refinery staff had on site only sufficient foam to fight a small fire, not fires associated with the breaching and ignition of a fuel tank.

Many of the 100+ tanks in the Tüpras refinery farm were constructed with floating roofs. Figures 4-15, and 4-17 are photographs of Tank 211, which is located immediately adjacent to many of the burned tanks (see Figure 4-18). Figure 4-17 is a photograph of the detail at the junction of the edge of the floating roof and perimeter wall, showing the perimeter seal. Sloshing of the fluid in the tank likely damaged the perimeter seal, which permitted the fluid to escape from the containment. Such observations have been made in other earthquakes (ASCE 1997). Oil evident on the top of the floating roof (Figure 4-17) spread over much of the roof. Danis (1999) reported substantial damage to a large number of tanks (30+) in the farm; the inability of perimeter seals to retain the sloshing fluid in the tanks resulted in failure or sinking of these floating roofs. Each of these damaged floating roofs required repair or replacement before the tanks could be returned to service. Repair of the damaged or sunken roofs would have involved draining the tanks, decontamination of the roof, and replacement of the perimeter seals.



Figure 4-15. Tank 211 in the Tüpras refinery tank farm



Figure 4-17. Perimeter seal of floating roof in Tank 211

Sloshing of fluid produced overtopping in several tanks (see Figure 4-19) and gross damage to the tank wall near the tops of walls in other tanks (see Figure 4-20). The oil lost from these tanks was contained within the earthen berms surrounding the tanks.

Members of the reconnaissance team found no evidence of substantial sliding of the tanks although none were anchored to their foundations. According to the refinery staff, this is typical practice in Turkish tank farms. Although hard piping was attached at the base of each tank, there was no evidence of pipe failure at any (unburned) tank visited by members of the team. Had there been appreciable movement of the tanks, many pipe failures would have occurred (ASCE 1997).



Figure 4-18. Partial view of Tupras tank farm showing Tank 211 and two burn zones



Figure 4-19. Overtopping of tank wall due to sloshing and failure of perimeter seals



Figure 4-20. View of tank wall damage



Figure 4-21. Photograph from top of Tank 211 facing south



Figure 4-22. Photograph from top of Tank 211 looking approximately south



Figure 4-23. Tank destroyed by fire in burn zone

Considered write-offs by the management (Danis 1999), approximately 20 tanks in the Tüpras refinery farm were damaged or destroyed by fire. Figures 4-21 and 4-22 are overlapping left-to-right photographs of burned tanks taken from the top of Tank 211 looking south toward the main processing facility. For reference, the mountains in the background of these photographs are located on the other side of Izmit Bay, to the south of the cities of Gölcük and Degirmendere. An overtopped tank can be seen to the left of the middle of Figure 4-21. Figures 4-23 and 4-24 are photographs of two tanks destroyed by fire. The tank in Figure 4-23 is located in tank burn zone 1 of Figure 4-18. The tank of Figure 4-24 is located in tank burn zone 2 of Figure 4-18. Twisted wreckage of the walls, walkways, and floating roof of the tank in Figure 4-24 can be seen in Figure 4-25. Figure 4-26 is a photograph of one tank, located immediately adjacent the burned tank of Figure 4-25 and linked to this tank by hard piping. Gross expansion of this fixed roof tank due to intense heating from the burning tank is evident. This tank can be seen to the right of the middle of Figure 4-22.



Figure 4-24. Tank destroyed by fire in burn zone



Figure 4-25. Destroyed walls, walkways and floating roof of tank in Figure 4-24



Figure 4-26. Gross expansion of fixed roof tank adjacent to tank of Figure 4-24

Although the Tüpras refinery tank farm suffered gross damage as a result of the fires following the earthquake, the damage could have been truly disastrous. The fire-fighting skills of the refinery staff and good decision making by the refinery management team kept these fires from spreading to other tanks on the farm and to adjacent industrial facilities, many of which

contained large amounts of volatile materials, such as the adjacent IGSAS plant that produces ammonia and fertilizer.

4.2.2.4 Main Processing Facility

The main processing facility is located between the tank farm and the loading jetty. An earthen berm and a road separate the facility from the tank farm. A total of four cooling towers, three made of wood and the fourth of reinforced concrete, were sited at the edge of the berm. One of the three wooden towers burned to the ground, another wooden tower was destroyed by earthquake shaking, and the third wooden tower suffered only slight damage. The reinforced concrete cooling tower appeared to be undamaged.

The main processing facility is composed of three crude-oil processing units. Constructed in 1983, one of the three units was destroyed by the collapse of an approximately 110-m-tall reinforced concrete heater stack in the middle of the unit. Figure 4-27, a photograph of the failed heater stack, was taken from the end of the loading and unloading jetty. The upper two thirds (approximately) of the heater stack collapsed. Failure of the stack likely initiated at a stiffness discontinuity in the reinforced concrete stack where large-size ductwork entered the stack. (See the undamaged heater stack to the left of the collapsed stack. Large-size ductwork enters this stack at approximately the same level at which the collapsed stack failed.) The top of the stack fell into a heater unit (Figure 4-28) and the lower portion of the failed stack collapsed onto pipework at the perimeter of the facility (Figure 4-29). Refinery staff reported that some pipework was fractured by the collapsing heater stack, which ignited fires in the crude-oil unit. These fires buckled structural components that supported the furnace and the pipeways.

The reconnaissance team did not observe any substantial damage to other parts of the main processing facility. Typical steel and reinforced concrete framing in the facility are shown in Figures 4-30a and 4-30b.



Figure 4-28. Damage to heater unit caused by collapse of heater stack



Figure 4-29. Damage to pipework caused by collapse of heater unit



Figure 4-30a. Undamaged steel-braced framing, Tupras refinery



Figure 4-30b. Undamaged reinforced concrete framing, Tupras refinery



Figure 4-31. Collapsed wooden cooling tower at the Petkim petrochemical facility



Figure 4-32. Damage to nonductile reinforced concrete in Petkim cooling tower

4.2.3 Petkim Petrochemical Plant

The Petkim (or Yarimca) petrochemical facility at Körfez is one of the largest state-owned facilities in Turkey. Similar to the Tüpras refinery, the Petkim facility supplies many industrial facilities in the region in and around Körfez, including a number of companies manufacturing components of tires. The Petkim petrochemical facility was constructed between 1965 and 1975; the main plant in the facility was fully operational in late 1969.

Parts of the Petkim facility were severely damaged. Maximum accelerations of approximately 0.32g were recorded at the YPT station (see Chapter 1), which was located within 200 m of the collapsed three-cell tower. Figure 4-31 shows the complete collapse of an older three-cell wooden cooling tower; but a four-cell tower adjacent to the collapsed tower suffered no damage. A reinforced concrete cooling tower approximately 400 m from the YPT station was badly damaged. Nonductile reinforced concrete columns at the perimeter of the cooling tower and atop a continuous reinforced concrete perimeter were severely damaged at the bases (Figure 4-32). Figure 4-33 shows typical damage and rebar details at the base of one column. The column in this figure was constructed with round longitudinal rebar. The transverse ties were widely spaced and 90° hooks were employed. It is evident in the figure that the transverse ties failed leading to dilation and failure of the core concrete in the *hinge* zone.



Figure 4-33. Rebar details and damage in reinforced concrete cooling tower at Petkim



Figure 4-34. Loading and unloading facility, Petkim petrochemical plant



Figure 4-35. Failure of battered reinforced concrete piles beneath jetty, Petkim facility

The Petkim petrochemical plant, similar to the Tüpras refinery, had a dedicated port facility through which much of the plant's raw material and processed product passed. Ground failure was observed near the jetty entrance. This port, like the port that serviced the Tüpras refinery, was badly damaged by the earthquake and was not operational afterward. Many of the battered piles beneath the jetty (Figure 4-34) were badly damaged. Typical damage to these battered piles is shown in Figure 4-35.

4.3 Automotive Industry

4.3.1 Introduction

Ford, Hyundai, and Toyota operate motor vehicle assembly plants in the epicentral region. Multinational industrial companies including Pirelli and Goodyear are located east of Izmit within a few miles of each other in the Köseköy and Alikahya regions. The Sabancı company has several joint-venture facilities in the epicentral region, including BekSA (a joint venture with Bekaert of Belgium), BriSA (a joint venture with Bridgestone, Japan, to manufacture rubber goods and tires), DuSA (a joint venture with Du Pont, USA), EnerjiSA, and KordSA. All of these companies contribute in one form or another to the construction of motor vehicles or components. With the exception of EnerjiSA, which is discussed in the following section, information on those facilities visited by the members of the reconnaissance team follows.



Figure 4-36. Framing of new body shop in Ford plant near

4.3.2 Ford Assembly Plant

The body-shop building of a new Ford plant near Gölcük was under construction at the time of the earthquake. The single-story building was composed of 6-m-tall square reinforced concrete columns supporting one-way steel trusses and a lightweight space frame spanning between the trusses. The roof and walls were constructed of lightweight steel panels. Figure 4-36 is a photograph of the interior of the new body shop.

This building was damaged during the earthquake by a combination of shaking and fault rupture and ground failure beneath the building. Figure 4-37 shows the degree of ground movement within 100 m. Damage included permanent deformations in the building frame, hinges in the cantilever columns (Figure 4-36), badly cracked and separated floor slabs, and collapse of some wall panels. Figure 4-38 shows the damaged building.



Figure 4-37. Ground movement near Ford plant, Gölcük



Figure 4-38. Exterior view of damaged Ford body shop

4.3.3 Hyundai Assembly Plant

The Hyundai plant located in Alikahya opened in late 1997. The lateral force-resisting system in the plant was composed of steel moment-resisting frames supported on a 0.6-m-deep raft foundation. The roof was constructed using a steel space frame and galvanized steel roof panels. Hyundai representatives reported that tensioned bolts in several column-to-roof truss connections sheared. Nonstructural mechanical and electrical components in a utility penthouse, approximately 9 m above ground level, suffered severe damage that included separations of elevated ducts from air handlers, movement of air handling units due to inadequate or no anchorage, and collapse of large-size ducts and cable trays due to inadequate attachments and anchorage.

4.3.4 Toyota Assembly Plant

The Toyota factory, which is located about 40 km west of Izmit in Adapazari, was constructed in 1994 with an annual vehicle production capacity of 100,000 cars. The lateral force-resisting system in the main plant building was composed of steel moment-resisting frames. Many of the columns in the building were jumbo shapes with flange thicknesses of up to 125 mm. Each column in the main building is supported on twelve 400-mm-diameter piles driven to rock at a depth of 14 m. Approximately 3,800 piles were driven beneath the building. No structural damage was observed in this building but nonstructural damage was widespread, including the failure or collapse of skylights, light fixtures, storage racks, and one substation transformer. Ground movement damaged the parking lot approximately 100 m from the main plant, the waste treatment plant. No structural damage was observed in other buildings or facilities visited by the reconnaissance team.

4.3.5 Pirelli Tire Plant

The Pirelli tire plant in Izmit consists of approximately 20 interconnected buildings, with a total floor area of more than 200,000 m² according to Pirelli representatives. The oldest construction dates back to the 1960s. One section of the oldest building in the plant, whose lateral force-resisting system was a nonductile reinforced concrete moment frame, collapsed killing one person and injuring 20. Modest-to-severe structural damage was reported in other buildings in the facility, including hinging of reinforced concrete columns. Nonstructural damage was widespread and included fallen light fixtures and cable trays.

The key pieces of equipment in the plant were Banbury extrusion machines, which process all raw elastomeric materials in the plant. Although these machines were undamaged by the earthquake, Pirelli representatives noted that these machines could not be restarted because of the degree of structural and nonstructural damage to the buildings where the machines were located, and they could not be easily moved elsewhere in the plant due to their size.

4.3.6 Goodyear Tire Plant

The Goodyear plant, a 500-person factory in Izmit at the time of the earthquake, is a steel-frame plant built in 1963. Only modest nonstructural and contents damage was observed, including collapse of light fixtures and localized failures of the fire-protection system that doused building contents with water. The reconnaissance team did not observe any structural damage in the office buildings.

4.3.7 BekSA

BekSA was established in 1987 and is apparently the largest independent steel wire manufacturer in the world. (The steel wire or cord is a key component in tires, bead wire, hose wire and spring wire.) The 57,000 m² BekSA plant (Figure 4-39) was partially operational ten days after the earthquake. The plant and the office buildings (to the left of the plant building in the photograph) were constructed of reinforced concrete. The main plant building suffered no apparent structural damage, but some nonstructural damage occurred including breakage of the windows at the top of the perimeter infill walls and cracking of infill masonry walls. One of the reinforced concrete framed office buildings collapsed completely. Many of the nonductile reinforced concrete columns in the main office building failed in shear but did not lose their ability to carry modest gravity loads.



Figure 4-39. BekSA plant

4.3.8 DuSA

The DuSA plant in Alikahya exports tire cord fabric and nylon yard, which are a key components in the production of automotive tires and industrial fabrics. The framing in the main plant building was a precast reinforced concrete frame supported on a 1-m-thick raft foundation. The reconnaissance team was not permitted to enter the main plant building. Heavy damage was reported by DuSA representatives and observed by the team. Figure 4-40 is a photograph of the perimeter of the main plant building that shows a partial collapse of the main building and unseating of precast beams from the corbels on the precast reinforced concrete columns. Substantial nonstructural damage was reported by DuSA representatives, including the failure of a continuous hot-process unit, equipment movement, overturning due to anchorage failures, and fracture of pipes due to relative movement of equipment.



Figure 4-40. Damage to the DuSA main plant building

A new steel-frame building was under construction at the time of the earthquake. Photographs of the framing were presented earlier in Figure 4-7. The structural frame suffered no damage. No damage was observed to nonstructural components in (ductwork and process equipment) and around (unanchored tanks and piping) of the new building.

4.3.9 KordSA

KordSA is a large producer of tire-cord fabric and industrial fabric. KordSA representatives reported that the plant was 50% operational one week after the earthquake. The main plant building (Figure 4-41) was constructed in 1973 with braced steel framing in the tower and precast reinforced concrete framed construction elsewhere. Only minor structural damage was observed in the tower, with buckled steel braces and damaged bolted connections. (No photographs were permitted by KordSA inside the main plant building.) The precast reinforced concrete framing in the main plant building suffered little-to-no structural damage (Figure 4-42). Some of the parapets atop the precast framing collapsed, as can be seen in the photograph. Only modest nonstructural damage was observed in the interior areas visited by the reconnaissance team.



Figure 4-41. KordSA main building showing steel braced-framed tower



Figure 4-42. Perimeter of precast reinforced concrete framed KordSA main plant building

A product storage area was added to the main plant after the original construction. The light steel-framed roof of this storage area collapsed (Figure 4-43), likely due to the differential movement of two parallel walls, also visible. A number of the *short* columns in the wall to the right failed in shear. The masonry infill above these short columns fell through the roof of the storage area.



Figure 4-43. Roof collapse in storage area of KordSA plant

4.4 Power Generation and Transmission Systems

4.4.1 Introduction

The seismic vulnerability of substation equipment and the damage experienced by power generation and transmission systems in the epicentral region was of much interest to PEER. The EnerjiSA power generation facility was visited by the reconnaissance team 11 days after the earthquake. Summary information on EnerjiSA is presented in Section 4.4.2. The loss of the substation at Adapazari, one of the key substations in the epicentral region, substantially hampered recovery efforts in the first few days following the earthquake. Much effort was focused on restoring the substation to service as quickly as possible. The substation was back in service before the reconnaissance team visited the substation ten days after the earthquake. Information on the observed damage in the Adapazari substation is presented in Section 4.4.3.

4.4.2 Power Generation

EnerjiSA supplies electricity and processed steam for selected Sabanci companies, including BriSA, ToyotaSA, KordSA, DuSA, and BekSA. EnerjiSA began production in 1997 as a 40-MW single-unit power plant. At the time of the earthquake, EnerjiSA was bringing online a 130-MW power unit and an additional 160 ton/hr of steam-generation capacity.

Transformers in the EnerjiSA facility were mounted on rails to facilitate installation and maintenance. Simple braking mechanisms were used to prevent movement of the transformers



Figure 4-45. Topped transformer in EnerjiSA transformer yard

and protect the equipment that is attached to the transformer such as bushings. Figure 4-44 shows one of the rail-mounted transformers in the EnerjiSA transformer yard. Movement along the rails of each transformer in the yard was observed. The typical movement, ranging between 50 and 100 mm, was most likely too small to endanger the interconnected equipment. However, one transformer, which was not in service at the time of the

earthquake, rolled or slid more than 1 m, dropped off the ends of the two support rails, and overturned (Figure 4-45). Two low-voltage

bushings failed during the earthquake and had been replaced by the time the reconnaissance team visited EnerjiSA.

A heat-recovery steam boiler (Figure 4-46a) that had been installed but not brought online at the time of the earthquake slipped off its foundation during the earthquake. The fillet welds joining the boiler framing to the base plates atop the reinforced concrete foundation failed (Figure 4-46b); these welds were small and of very poor quality.

The base plate connections of steel framing to components of both the existing and the new steam generation systems failed. Figure 4-47a shows two-level framing to an in-service chimney. Figure 4-47b shows the damage at the base plate connection. Figure 4-48a is a photograph of

steel braced framing in the new steam-generation system. Figure 4-48b shows damage to the grouted base plate connection and steel brace that was located on the far side of the steel bracing in Figure 4-48a. The shear key (Figure 4-48b) was not embedded in the concrete pedestal beneath the grout pad but in the grout pad only.

4.4.3 Power Transmission

The 380 kV substation in Adapazari services the city of Adapazari and surrounding townships and industrial facilities. The reconnaissance team visited the substation ten days after the earthquake by which time much of the damaged hardware had been replaced by components stockpiled at the substation and in Ankara.



Figure 4-46a. Damaged boiler, EnerjiSA plant



Figure 4-46b. Failed fillet-weld connection of boiler framing to baseplate



Figure 4-47a. Damage to steel framing to EnerjiSA in-service steam generator



Figure 4-47b. Damaged baseplate connection, EnerjiSA in-service steam generator

An aerial photograph of the substation is shown in Figure 4-49. Much switching gear and two power transformers can be seen in the photograph. Numerous porcelain insulators failed during the earthquake; some of the fractured units can be seen in Figures 4-50a and 4-50b. Figure 4-51 is a view of pre- and post-earthquake-installed circuit breakers in the substation; rigid bus connectors span the service road. The V-headed shaped circuit breakers were in service at the time of the earthquake. The T-headed circuit breakers replaced the failed V-headed circuit breakers and had been installed well prior to the visit by the reconnaissance team. Those V-

headed circuit breakers that failed during the earthquake typically had longer runs of interconnected equipment than those V-headed circuit breakers that survived the earthquake.



Figure 4-48a. Damaged framing to new steam generator, EnerjiSA



Figure 4-48b. Failed fillet weld connection of new boiler framing to baseplate, EnerjiSA



Figure 4-49. Aerial view of the Adapazari substation

V-headed gas circuit breakers from a number of manufacturers were in service at the time of the earthquake. Many of the cantilever ABB circuit breakers failed during the earthquake. None of the braced Hitachi circuit breakers of Figure 4-52 were damaged.

The substation staff reported that no bushings failed during the earthquake. The reconnaissance team also found no evidence of failed transformer bushings. The power transformers of Figures 4-53a and 4-53b were carefully inspected for damage; no damage was found. The brakes on these rail-mounted transformers failed to function during the earthquake; the maximum movement of these transformers was approximately 300 mm. Such movement appeared not to damage the transformers, the transformer bushings, or the interconnected equipment.



Figure 4-50a. Failed porcelain insulators



Figure 4-50b. Failed porcelain circuit breakers



Figure 4-51a. View along service road showing pre- and post- earthquake circuit breakers



Figure 4-51b. New T-shaped circuit breakers



Figure 4-52. Braced Hitachi gas circuit breaker, Adapazari substation



Figure 5-53a. Elevated support frames and power transformers, Adapazari substation



Figure 4-53b. Power transformer, Adapazari substation

4.5 Other Heavy Industry

4.5.1 Bastas Plant

Bastas manufactures fluorescent lightbulbs. Although the plant suffered no structural damage from the earthquake and power was available immediately after the earthquake using on-site emergency generators, nonstructural damage to a glass furnace forced the shutdown of the plant. The furnace was mounted on an unanchored frame that moved approximately 35 mm.

Compressed air to the furnace was lost when a valve was damaged on a temperature-control rack. The resulting change in the fuel-air mixture led to molten brass solidifying in the lines of the furnace and the destruction of a custom-made tube in the furnace. The lead-time to replace the custom-made tube was at least six to eight weeks, forcing the plant to close for this time because the tube was key to the function of the furnace and the plant.



Figure 4-54 Collapsed precast reinforced concrete building, Cap textile plant.

4.5.2 Çap Plant

The Çap textile facility is located 3 km west of Akyazi, which is east of Adapazari, on alluvium deposits between two rivers that are 500 m apart near the plant. The plant was composed of two 3-bay (transverse) by 15-bay (longitudinal) precast reinforced concrete buildings. The framing of the two buildings appeared to be most similar. The typical interior column was 6 m high and 250 mm by 600 mm in plan, with the strong direction of the column in the transverse direction. Figure 4-3b is part of the transverse cross section in the building. One of the two precast buildings collapsed (Figure 4-54). The second building suffered severe damage. In this precast building, many of the columns hinged at the bases, and wall and roof panels collapsed.

4.5.3 Habas Plant

The Habas plant in Izmit provides liquefied gases to commercial plants and medical facilities in the Izmit and surrounding regions. The major damage at Habas was the collapse of two of the three liquid gas storage tanks shown in Figure 4-55.

Three identical 14.63-m-diameter tanks were built in 1995. Each tank consisted of two concentric stainless steel shells, one with an outside diameter of 14.63 m and the other with an outside diameter of 12.80 m. Figure 4-56 is a photograph of the undamaged tank. The gap between the shells is filled with insulation. Both shells were supported on a 14.63-m-diameter, 1.07-m-thick reinforced concrete slab that was in turn supported by sixteen 200-mm-diameter reinforced concrete columns. Each column was 2.54 m in height and reinforced with 16 No. 16-mm-diameter longitudinal bars and 8-mm-diameter ties at 100 mm on center.



Figure 4-55. Liquid gas plants at the Habas plant



Figure 4-56. View of Reinforced concrete framing at base of undamaged tank, Habas plant

The two tanks containing liquid oxygen collapsed as seen in Figure 4-57. The tank and supporting structure containing liquid nitrogen was undamaged except for some hairline cracks in the columns. Habas representatives reported that the liquid oxygen tanks were 85% full, and the liquid nitrogen tank was 25% full at the time of the earthquake. The outer shells of the collapsed tanks buckled (Figure 4-58). Photographs of some of the failed columns beneath one of the liquid nitrogen tanks are presented in Figure 4-59.



Figure 4-57. Collapse of liquid oxygen tanks



Figure 4-58. Buckling of the outer stainless steel shell in liquid oxygen tank



Figure 4-59a. Failed columns beneath slab under liquid oxygen tank, Habas facility



Figure 4-59b. View of failed columns beneath liquid oxygen tank, Habas facility

4.5.4 Mannesmann Boru Plant

The Mannesmann Boru steel-pipe plant in Izmit was constructed in the mid-1950s. The plant is composed of two separate facilities for the fabrication of small- and large-diameter pipe. Each facility includes production buildings and warehouses. An administration building and storage yards are common to both facilities.



Figure 4-60a. Undamaged crane at

Damage was observed in reinforced concrete and steel buildings. In two buildings, shear cracking was prevalent in nonductile columns with short shear spans due to the presence of infill masonry walls. In one of the large-pipe production buildings, the anchor bolts of a steel moment-resisting frame elongated and fractured. In the storage yard at the large-pipe area, two cranes that were constructed in the early 1970s suffered identical failures of the box sections supporting one leg of the crane. Figure 4-60a is a photograph of an undamaged crane in the yard. Figure 4-60b shows the failed leg of another crane in the yard.

Mannesmann Boru used the adjacent SEKA paper-mill port facility for



Figure 4-60b. Collapsed crane leg, Mannesmann Boru pipe storage facility

handling raw materials and pipe product. As discussed in the following section, the SEKA port facility was badly damaged in the earthquake, forcing Mannesmann Boru to use alternative and less efficient methods for moving raw materials and product.

4.5.5 SEKA Plant

SEKA is a state-owned paper mill that is located next to the Mannesmann Boru plant. Paper and cardboard products are produced and processed in this plant, which includes five paper mills, each with two paper machines. Before the earthquake, SEKA moved raw materials and finished product through its port facility. The SEKA port facility is composed of two separate jetties, both of which failed during the earthquake. Figure 4-61a shows one of the two jetties that were supported on hammerhead reinforced concrete columns that were constructed in the 1960s. The influence of the horizontal framing immediately above the waterline on the failure of the hammerhead columns is not known. Figure 4-61b is a photograph of the second jetty that is of reinforced concrete construction like the jetty of Figure 4-61a but with substantially different framing. The jetty of Figure 4-61b was also severely damaged with one section of the jetty dropping more than 300 mm below the adjacent sections.

Three reinforced concrete silos containing water collapsed. Figures 4-62a and b are photographs of an undamaged and a collapsed silo, respectively. The diameter of the silos was approximately 6 m. The collapsed silos were supported on six small square nonductile columns with minimal longitudinal reinforcement. The undamaged silos of Figure 4-62a were supported on larger (square) columns than those of the collapsed silos.



Figure 4-61a. Failure of hammerhead reinforced concrete jetty piers, SEKA paper mill



Figure 4-61b. View of failed jetty, SEKA paper mill



Figure 0-14-62a. Undamaged silo at SEKA paper mill



Figure 4-62b. Collapsed silo, SEKA paper mill

4.5.6 Liquid Gas Tanks

Cylindrical (bullet) liquid gas tanks of the type shown in Figure 4-63 were common in the Körfez industrial parks. Most of the tanks of this type were not anchored and had hard pipe connections of the type seen in Figure 4-63b. These connections are most susceptible to damage due to movement and rotation of the tank with respect to the supporting saddle. Movement and rotation of the tank with respect to the pedestal are clearly evident in Figure 4-63b.

Many spherical liquid petroleum gas (LPG) tanks were located in the epicentral region in a large number of industrial facilities. These tanks were typically supported by braced steel frames or reinforced concrete frames. No damage to these tanks was observed by members of the reconnaissance team.



Figure 4-63a. Typical support arrangement for cylindrical liquid gas tanks



Figure 4-63b. Typical damage to liquid gas tanks

5 Summary and Conclusions

5.1 Summary

A team of structural engineers representing the Pacific Earthquake Engineering Research (PEER) Center visited the area affected by the August 17, 1999, Izmit earthquake in late August and early September 1999. The M_w 7.4 earthquake occurred on the North Anatolian fault in northwestern Turkey at 3:02 a.m. local time. The hypocenter of the earthquake was located near Izmit, 90 km east of Istanbul. Official figures placed the loss of life at 17,225, with more than 44,000 injured. Approximately 77,300 homes and businesses were destroyed and 245,000 were damaged. The total direct loss was estimated to be more than US\$ 6 billion.

The PEER reconnaissance team traveled to Turkey to study damaged and undamaged buildings, bridges, industrial facilities, and infrastructure. Two key objectives of the reconnaissance effort were (1) to improve the understanding of the *performance* of the built environment and (2) to identify gaps in the PEER research agenda, which is developing knowledge and design tools for performance-based earthquake engineering. Documenting collapsed structures was not a high priority of the reconnaissance team, and no such documentation is provided in this report.

This report begins with an introduction to building seismic design and construction practice in the region impacted by the earthquake, and follows with a description of the performance of damaged and undamaged structures. The review of design and construction practice (Chapter 2) confirmed that the construction of reinforced concrete buildings without special details for ductile response (by far the most prevalent form of construction in the epicentral region) was permitted up to the time of the earthquake.

The performance of reinforced concrete frame and wall buildings is presented in Chapter 3. Typical construction practice did not make use of special details for ductile component behavior because (a) the use of special details was not mandated by the codes of practice or local authorities and (b) buildings without the special details were easier to construct. Construction quality varied widely and ranged from excellent to poor. The quality of residential construction was typically moderate to poor. The performance of components of moment-frame buildings (beams, columns, joints) and wall buildings is described. Much of the observed poor performance was directly related to the use of (a) nonductile reinforcement details and (b) inappropriate framing sizes (e.g., strong beams and weak columns). Another key contributor to poor building

performance was widespread ground failure or liquefaction that likely protected some buildings from severe earthquake shaking but which resulted in gross building settlement or overturning. A detailed discussion on the performance of four buildings is presented in Section 3.5. Components of three of the four buildings were either severely damaged or destroyed but none of these buildings collapsed. The effect of component failure on system response is studied in this section, and issues related to preventing collapse of gravity-load-resisting frames are explored.

Chapter 4 presents information on the performance of industrial facilities. Because many of these facilities were designed in the 1960s and 1970s using U.S. or European codes of practice, and given that the construction quality in these structures was typically good to excellent, the performance of these older facilities during the August 17 earthquake could be considered to be representative of that of industrial facilities of a similar age in the United States and Europe. Of particular relevance to facility operators in the United States was the performance of the Tüpras refinery and the life-threatening problems faced by the refinery staff immediately following the earthquake. One important lesson from the Tüpras experience is that earthquake preparedness is key to rapid response and timely recovery.

5.2 Conclusions and Recommendations

A short list of conclusions and recommendations related to design and construction practice in Turkey is enumerated below.

1. Nonductile detailing should not be allowed in moderate and severe seismic zones, regardless of the lateral forces used for design.
2. A factor that accounts for the proximity of a building site to a fault (i.e., a near-field factor) should be included in the design force equation.
3. Construction on ground prone to liquefaction should be avoided.
4. Building frames that have been designed for gravity loads alone, and without a clear load path for lateral loads, should be treated as a high priority for retrofitting.
5. Continuous shear walls on stiff and strong foundations are an effective means of retrofitting nonductile reinforced concrete buildings. Existing independent column foundations should be tied together with grade beams in retrofit construction.
6. In new and retrofit reinforced concrete construction, smooth reinforcing bars should not be used other than for stirrups and ties.
7. Careful attention should be paid to concrete mix design, quality control, and placement.

The work and observations of the reconnaissance team raise many questions related to the performance of reinforced concrete buildings and the implementation of performance-based earthquake engineering in the United States and abroad. Some of the important questions are

1. Why do apparently similar buildings subjected to apparently similar earthquake shaking perform very differently? What are the determining features that differentiate their behaviors?
2. What are the causes of collapse in gravity-load-resisting frames? Can we better capture the effect of component failure on system response? Can we develop gravity-load-framing systems that are less prone to collapse?
3. Can we better characterize the effect of ground failure on earthquake ground motion? Can cost-effective methods for ground improvement be developed for new and retrofit construction?
4. Why did some buildings within meters of the fault, or in some cases straddling it, survive with little to no damage, while others of apparently similar construction but further from the fault collapse? Is earthquake shaking very close to the line of rupture less severe than that a short distance from it?

Appendix: Performance of the Adapazari City Hall

A.1 Introduction

Construction of Adapazari City Hall was started in 1959 and completed in 1964. This five-story reinforced concrete frame building was heavily damaged during the July 22, 1967, Akyazi M7.1 earthquake and retrofitted using conventional methods in the eight-month period after that earthquake. Adapazari was 36 km east of the epicenter of the 1967 earthquake. The estimated intensity in Adapazari was MMI 7.

The building is located in downtown Adapazari where many buildings either collapsed or suffered substantial damage during the August 17, 1999, Kocaeli earthquake. Since the retrofitted building suffered only minor damage, it was used as the headquarters of the city crisis center to direct earthquake-relief efforts. Aftershocks of the August 17 earthquake and the main shock of the November 12, 1999, Duzce M7.2 earthquake caused existing cracks to open more and new cracks to form in the frame members and infill walls.

A.2 Background Information

Like most other buildings in Adapazari, the City Hall building does not have a basement, since the water table lies 1 to 2 m below grade. The building is located on relatively soft soil deposits (Anadol et al. 1972). The foundation is composed of tapered footings (Figure A-1) connected with 400 mm by 900 mm grade beams in the x (longitudinal) direction and 500 mm by 1500 mm base beams in the y (transverse) direction.

The building has a clear height of 17 m above ground level. The plan footprint is 14.2 m by 40 m with 13 frames in the transverse direction and 3 frames in the longitudinal direction. A typical floor plan and elevation in the original structure are shown in Figure A-1. The shear walls in the transverse direction were not placed symmetrically in plan and created a stiffness eccentricity of 3.7 m. Anadol et al. (1972) reported that the concrete strength was 16 MPa (2350 psi) and that the yield strength of the smooth reinforcing bars was 220 MPa (32 ksi).

Resistance to lateral forces in the original structure was provided by two shear walls and 35 columns. The depth of the columns varied between 300 mm and 700 mm, and the width varied between 230 mm and 400-mm. Typical floor framing consisted of a 370-mm-deep joist system infilled with lightweight bricks, and 370-mm-deep beams varying in width from 400 mm to 1000 mm. The lightweight brick infill walls, which ranged between 100 mm and 150 mm in thickness, were not designed to carry lateral or gravity loads. Light steel sections were welded to the window frames at each story level on the facade. These steel sections were not part of the gravity- or lateral-load-resisting system.

A.3 1967 Akyazi Earthquake: Damage and Bung Retrofit

The damage observed after the 1967 M7.1 Akyazi earthquake was concentrated in the shear walls (Figure A-2) and columns in the lower stories. As shown in Figure A-3a, no ties were observed in one column (Grid A-1 in Figure A-1). In this figure "Etriye yok" translates as "No tie." Figure A3b shows shear failure in a column; this column was located at Grid T4 in the basement. Damage to stairwells, slabs, and beams was also reported at several floors. Large shear cracks were observed in many of the infill walls.

The 1967 retrofit program included repair and strengthening of damaged slabs, beams, columns and shear walls, and the addition of new beams and shear walls. Columns were typically retrofitted by the addition of transverse reinforcement and an increase in the column size by 140 mm to 180 mm. New transverse perimeter shear walls were added on Grids 1 and 13, and transverse interior shear walls were added on Grids 8, 9, and 10 to match existing walls on Grids 4, 5, and 6. Short longitudinal walls were placed in the four corners of the building. Figure A-4 shows the locations of the new reinforced concrete shear walls. ("B.A. perde" translates as "RC shear wall"). Existing perimeter longitudinal beams were retrofitted and new perimeter longitudinal beams were added as indicated in Figure A-5. The new longitudinal walls are shown hatched in this figure.

The fundamental periods of the building were calculated to be 1.38 and 1.08 sec in the longitudinal and transverse directions, respectively (Anadol et al 1972). After the retrofit work had been completed, the periods of the building were measured at 1.10 sec and 0.31 sec in the longitudinal and transverse directions, respectively (Aytun 1972). A summary of the building characteristics before and after retrofitting is given in Table A-1.

Table A-1 Characteristics of Adapazari City Hall (Anadol 1972)

	<i>Original building</i>	<i>Retrofitted building</i>
Average soil pressure	7.20 ton/m ²	7.92 ton/m ²
Strength of the building	Stronger in the v direction	Almost equal in both directions
Fundamental period (x-dir)	1.38 sec	1.10 sec
Fundamental period (v-dir)	1.08 sec	0.31 sec
Total weight	4370 tons	4732 tons
Stiffness eccentricity	$e_x=17.7\%, e_v=14.2\%$	$e_x=0\%, e_v=1.1\%$
Estimated ductility	1.5-2.0	4
Lateral force coefficient	C=0.04	C=0.07

A.4 1999 Kocaeli Earthquake and Aftershock

The North Anatolian fault ruptured within 10 km of the City Hall and devastated many reinforced concrete moment-frame buildings in the immediate vicinity of the City Hall, but this retrofitted building sustained negligible structural damage. The nonstructural components and contents suffered only modest damage. Because the City Hall was one of the few buildings in downtown Adapazari that suffered little to no structural damage, it was used as an Emergency Crisis Center to direct response and recovery after the earthquake. Figure A-6 presents two photographs of the City Hall taken in mid-November 1999.

The solid line in Figure A-7 presents the 5% damped pseudo-acceleration response spectrum prepared using the east-west ground acceleration history recorded a few kilometers from the City Hall during the August 17, 1999, earthquake. The zero-period acceleration for this recorded ground motion was 0.41g. The spectral acceleration at 1 sec, the approximate period of the City Hall building, was 0.4g. Because the building sustained little to no structural damage, and assuming that the strength of the building was no greater than 15% of the weight (calculated by doubling the allowable-stress-design lateral-force coefficient of 0.07), the intensity of shaking at the site of the building was likely substantially less than that indicated by the solid line in the figure. Parenthetically, the elastic spectral demands associated with the earthquake shaking in Adapazari were large, and it is not surprising that many nonductile reinforced concrete moment frame buildings in this city collapsed because the spectral demands greatly exceeded the lateral strength of these buildings that likely did not exceed 5% to 10% of their weight.

On November 11, 1999, an aftershock of the August 17 earthquake produced substantial shaking in Adapazari. The dashed line in Figure A-7 is the 5% damped pseudo-acceleration response spectrum prepared using the east-west ground acceleration history recorded at the site described in the previous paragraph. The zero-period acceleration for this motion was 0.35g. Additional damage to structural and nonstructural components in the City Hall was reported.

The lack of damage to the structural frame of the City Hall building, and the almost complete destruction of reinforced concrete moment-frame buildings around it clearly show that reinforced concrete walls are an effective means of retrofitting older reinforced concrete construction in Turkey. The strategic placement of new structural walls can reduce the plan and vertical irregularities of an existing building, thereby substantially improving its performance. The addition of a modest number of structural walls to the original City Hall building more than doubled the strength and substantially increased the stiffness of the building. The walls protected the vulnerable nonductile columns and joints from the gross damage and collapse that was observed in adjacent buildings.

A.5 Summary Remarks

The excellent performance of the retrofitted Adapazari City Hall in the August 17, 1999, main shock and the November 11, 1999, aftershock is, by comparison with the poor performance of most reinforced concrete moment-frame buildings in the immediate vicinity of the City Hall, a clear endorsement for retrofitting using reinforced concrete shear walls. The introduction of a modest number of strategically placed ductile structural walls into an existing nonductile reinforced concrete moment-frame building will protect the vulnerable nonductile components

and substantially improve the performance of the building. Such conventional methods of retrofitting are the most promising and cost effective means of reducing the vulnerability of the large inventory of nonductile moment-frame buildings in Turkey.

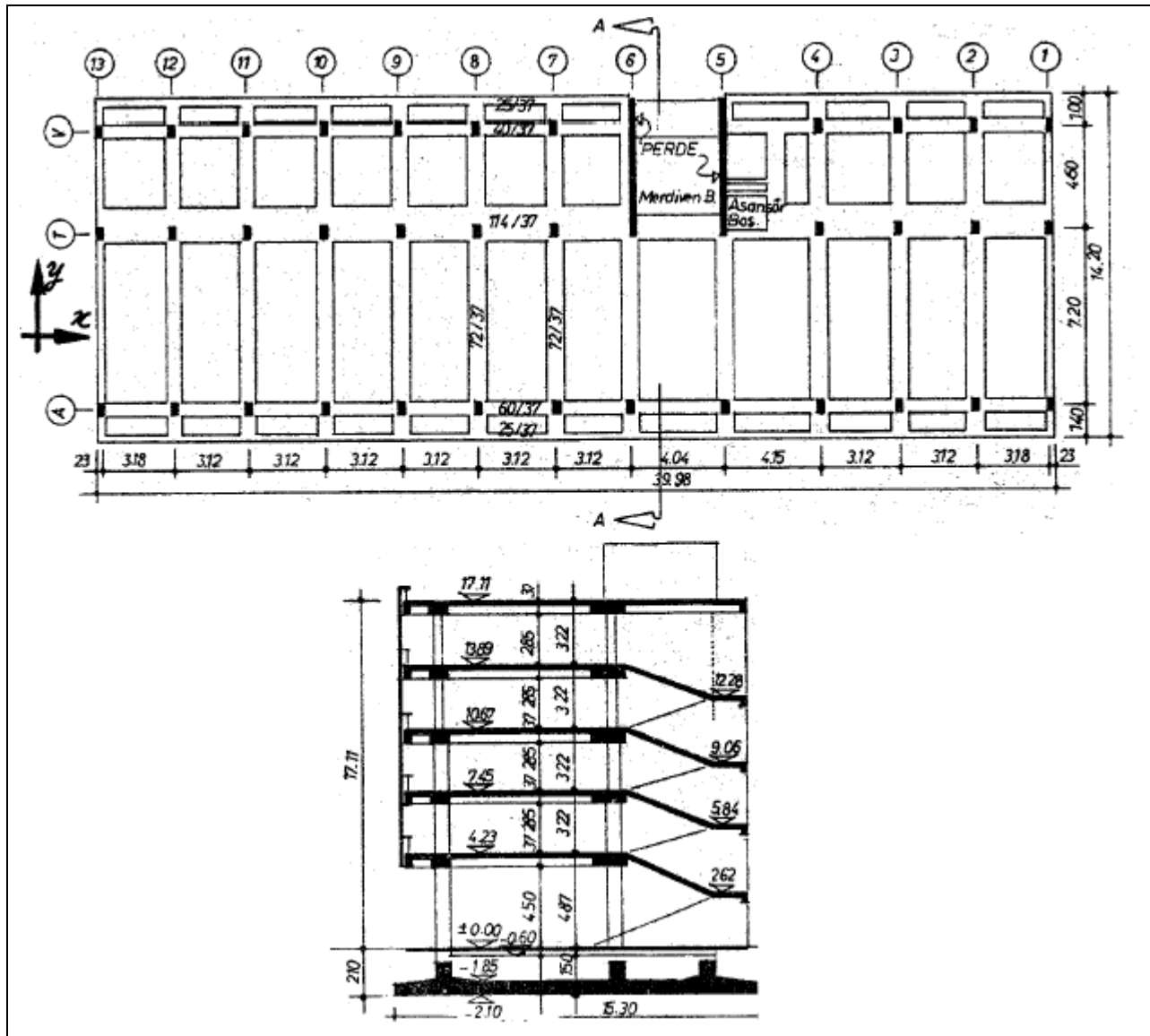


Figure A-1 Typical plan and elevation of the original building (Anadol et al. 1972)

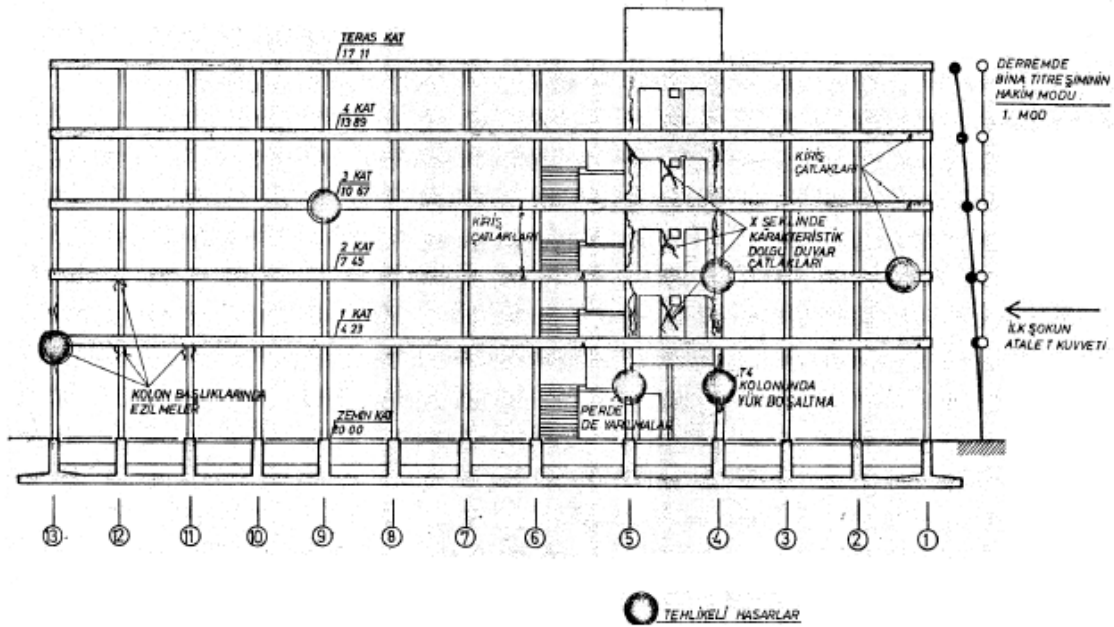
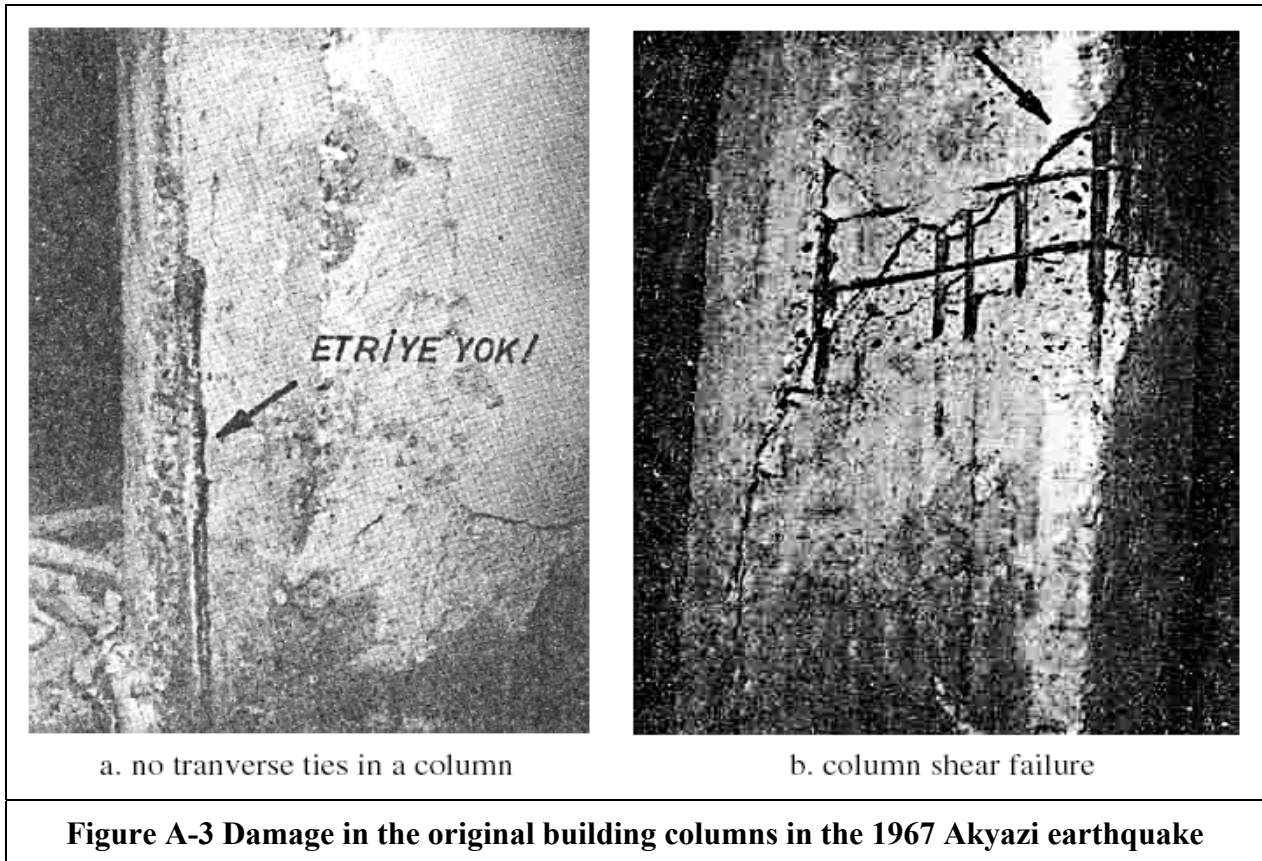


Figure A-2 Building damage after the 1967 Akyazi earthquake



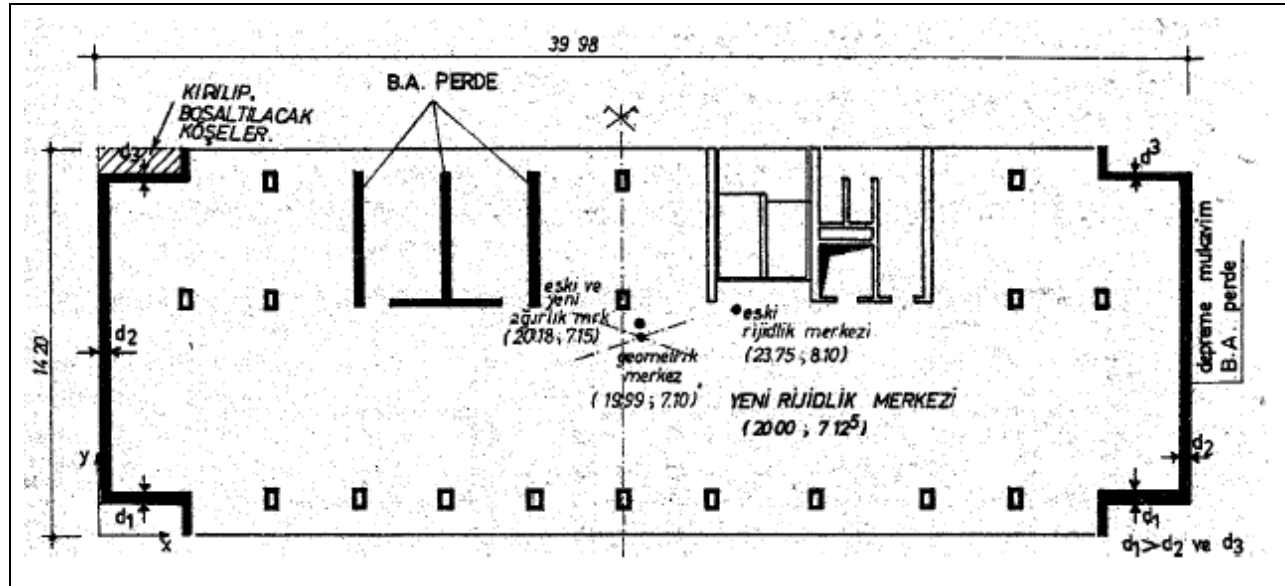


Figure A-4 Typical floor plan after retrofit showing the location of new shear walls (Anadol et al. 1972)

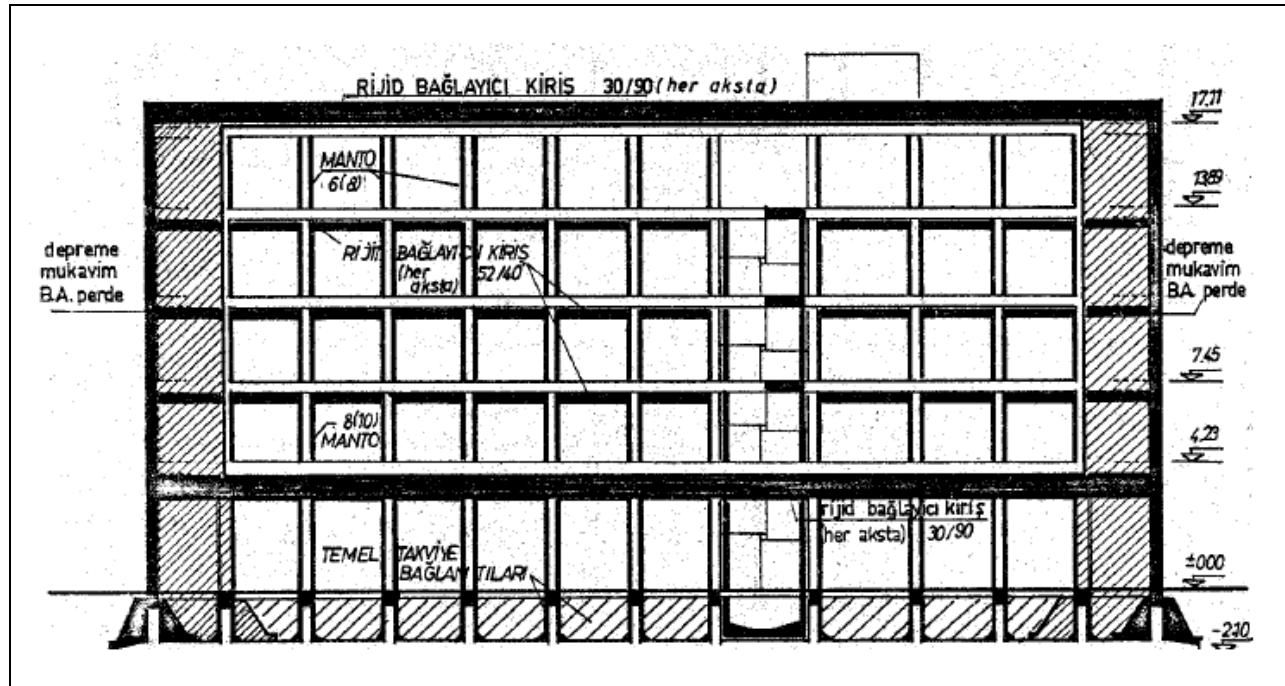


Figure A-5 Front elevation after the retrofit in 1968 (Anadol et al. 1972)



a. back view (V and 1 axes on plan, Fig. A-1)



b. front view (A and 13 axes on plan, Fig. A-1)

Figure A-6 City Hall after the November 12, 1999, Duzce earthquake

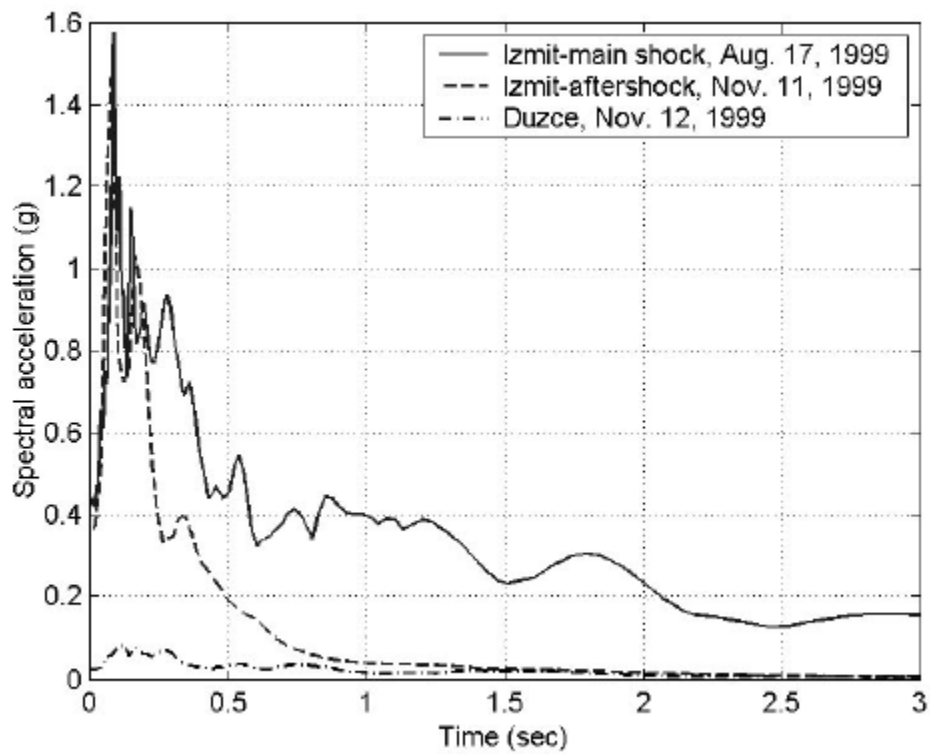


Figure A-7 Acceleration spectra for the August 17, 1999, Izmit main shock; the November 11, 1999, Izmit aftershock; and the November 12, 1999, Duzce main shock

References

ACI. 1999. *Building code requirements for structural concrete*. ACI 318-99. Farmington Hills, Mich.

American Society of Civil Engineers. 1997. *Guidelines for seismic evaluation and design of petrochemical facilities*. Reston, Va.: ASCE.

Anadol, K., U. Arioglu, and E. Arioglu. 1972. The restoration and reinforcing project of the Sakarya Municipal Building which was damaged during the 1967 Akyazi earthquake. In *Symposium on Earthquake Engineering and Earthquake Related Problems in Turkey*. Ankara, Turkey: Scientific and Technical Research Council of Turkey, Middle East Technical University. (In Turkish).

FEMA. 1997. *NEHRP guidelines for the seismic rehabilitation of buildings*. FEMA 273. Washington D.C.: [Federal Emergency Management Agency].

Applied Technology Council. 1995a. *Structural response modification factors*. Report ATC-19. Redwood City, Calif.: Applied Technology Council.

Applied Technology Council. 1995b. *A critical review of current approaches to earthquake resistant design*. Report ATC-34. Redwood City, Calif.: Applied Technology Council.

Aytun, A. 1972. Experimental determination of natural vibration periods of structures. In *Symposium on Earthquake Engineering and Earthquake Related Problems in Turkey*. Ankara, Turkey: Scientific and Technical Research Council of Turkey, Middle East Technical University. (In Turkish).

Bayulke, Nejat. 1992. Reedition history of seismic design code of Turkey. *Bulletin of the International Institute of Seismology and Earthquake Engineering* 26: 413–29.

Danis, Husamettin. 1999. General Manager. Turkish Petroleum Refineries Corp., Tupras. Personal communication.

Duyguluer, M. F. 1997. The history of seismic design code of Turkey. *Bulletin of the International Institute of Seismology and Earthquake Engineering* 31: 177–92.

Gulkan, P. 2000. Building code enforcement prospects: The failure of public policy. *Earthquake Spectra* 16 (Supplement A): 351–67.

International Association for Earthquake Engineering. 1966. *Earthquake resistant regulations: A world list*, pp. 307–18. Tokyo: Gakujutsu Bunken Fukyu-kai.

International Conference of Building Officials. 1997. *Uniform Building Code, volume 2, Structural engineering design provisions*. Whittier, Calif.: ICBO.

Ministry of Public Works and Settlement. 1997. *Specification for structures to be built in disaster areas, Part III—earthquake disaster prevention*. [Istanbul]: Government of Republic of Turkey.

Ministry of Public Works and Settlement. 1995. *Specification for structures to be built in disaster areas*. [Istanbul]: Government of Republic of Turkey.

Moehle J. P., K. J. Elwood, and H. Sezen. October 2000. Gravity load collapse of building frames during earthquakes. In ACI Special Publication *Behavior and design of concrete structures for seismic performance*. American Concrete Institute Fall 2000 Convention. Toronto: American Concrete Institute.

Turkish Standards Institute. 1985. *TS-500, building code requirements for reinforced concrete*. Ankara, Turkey.

Vision 2000. 1995. *Performance based seismic engineering of buildings*. Prepared by Structural Engineers Association of California. Sacramento, Calif.: [SEAOC].